

ผลเฉลยเชิงตัวเลขของสมการมัลติลินส์



นางสาวพัชรินทร์ ตระกูลศิริศักดิ์

สถาบันวิทยบริการ

จุฬาลงกรณ์มหาวิทยาลัย

วิทยานิพนธ์นี้เป็นส่วนหนึ่งของการศึกษาตามหลักสูตรปริญญาวิทยาศาสตรมหาบัณฑิต

สาขาวิชาวิทยาการคณนา ภาควิชาคณิตศาสตร์


คณะวิทยาศาสตร์ จุฬาลงกรณ์มหาวิทยาลัย

ปีการศึกษา 2545

ISBN 974-17-1408-4

ลิขสิทธิ์ของจุฬาลงกรณ์มหาวิทยาลัย

NUMERICAL SOLUTIONS TO MULLINS EQUATION



Miss Patcharin Tragoonsirisak

สถาบันวิทยบริการ
จุฬาลงกรณ์มหาวิทยาลัย

A Thesis Submitted in Partial Fulfillment of the Requirements
for the Degree of Master of Science in Computational Science

Department of Mathematics

Faculty of Science

Chulalongkorn University

Academic Year 2002

ISBN 974-17-1408-4

Thesis Title NUMERICAL SOLUTIONS TO MULLINS EQUATION
By Miss Patcharin Tragoonsirisak
Field of Study Computational Science
Thesis Advisor Assistant Professor Pornchai Satravaha, Ph.D.

Accepted by the Faculty of Science, Chulalongkorn University in Partial
Fulfillment of the Requirements for the Master 's Degree

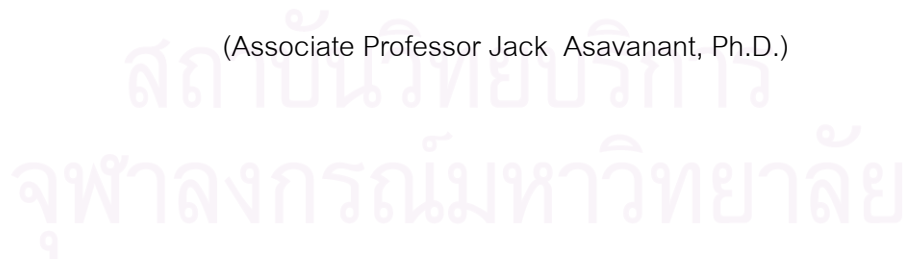
..... Dean of Faculty of Science
(Associate Professor Wanchai Phothiphichitr, Ph.D.)

THESIS COMMITTEE

..... Chairman
(Associate Professor Suchada Siripant)

..... Thesis Advisor
(Assistant Professor Pornchai Satravaha, Ph.D.)

..... Member
(Associate Professor Jack Asavanant, Ph.D.)



พัชรินทร์ ตระกูลศิริศักดิ์ : ผลเฉลยเชิงตัวเลขของสมการมัลลินส์ (NUMERICAL SOLUTIONS TO MULLINS EQUATION) อ. ที่ปรึกษา : ผู้ช่วยศาสตราจารย์ ดร.พรชัย สาตราหา, 80 หน้า. ISBN 974-17-1408-4.

สมการมัลลินส์เป็นสมการเชิงอนุพันธ์ย่อยไม่เชิงเส้นอันดับสี่ ซึ่งอธิบายการเกิดร่องบนขอบเกรนที่เกิดจากการแพร่บนพื้นผิว เราหาผลเฉลยของสมการมัลลินส์โดยวิธีการแปลงลาปลาซผสมผสานกับวิธีผลต่างสี่เหลี่ยม หรือเรียกโดยย่อว่าแอลทีเอฟดีเอ็ม ได้แสดงผลลัพธ์ในรูปของกราฟของพื้นผิว สำหรับความชันของร่องในช่วงระหว่าง 0 ถึง 4.5 เมื่อความชันที่ร่องไม่มากกว่า 0.7 ผลเฉลยเชิงตัวเลขที่หาได้สอดคล้องดีมากกับผลเฉลยที่ได้จากแบบจำลองซึ่งสามารถหาผลเฉลยได้ด้วยวิธีเชิงวิเคราะห์ของ Tritscher และ Broadbridge อย่างไรก็ตามรูปร่างของร่องยังคงถูกต้องแต่ความแม่นยำลดลงเมื่อเพิ่มความชันของร่องมากขึ้น

นอกจากนี้ เราได้ศึกษาเทคนิคเชิงตัวเลขวิธีอื่นอีกคือ การประมาณค่าโดยเส้นโค้งกำลังสามและผลต่างสี่เหลี่ยม จากการทดสอบเชิงตัวเลขของแต่ละวิธีพบว่า สำหรับผลเฉลยเชิงตัวเลขที่มีความแม่นยำเท่ากัน วิธีแอลทีเอฟดีเอ็มใช้เวลาน้อยกว่าวิธีอื่นมาก

สถาบันวิทยบริการ
จุฬาลงกรณ์มหาวิทยาลัย

ภาควิชา คณิตศาสตร์
สาขาวิชา วิทยาการคณนา
ปีการศึกษา 2545

ลายมือชื่อนิติ.....
ลายมือชื่ออาจารย์ที่ปรึกษา.....
ลายมือชื่ออาจารย์ที่ปรึกษาร่วม.....

4372349323 : MAJOR COMPUTATIONAL SCIENCE

KEY WORD: NON-LINEAR PDE / LAPLACE TRANSFORM / FINITE DIFFERENCE

PATCHARIN TRAGOONSIRISAK : NUMERICAL SOLUTIONS TO MULLINS EQUATION.

THESIS ADVISOR : ASSIST. PROF. PORNCHAI SATRAVAHA, Ph.D., 80 pp. ISBN 974-17-1408-4.

Mullins equation, the fourth-order non-linear partial differential equation describing grain boundary grooving by surface diffusion, is solved by Laplace transform finite difference method (LTFDM). The surface profiles for groove root slopes ranging between 0 and 4.5 are presented. The numerical results show excellent agreement with solutions obtained from Tritscher and Broadbridge's analytically solvable model when slope at the groove root is not more than 0.7. The shape of the groove is still correct, however, with less accuracy when increasing the groove slope.

Other numerical methods are also investigated, including cubic splines and finite difference methods. Our numerical test run of each method shows that, with the same accuracy of results, LTFDM uses time much less than the others.

สถาบันวิทยบริการ
จุฬาลงกรณ์มหาวิทยาลัย

Department **Mathematics**

Field of study **Computational Science**

Academic year **2002**

Student's signature.....

Advisor's signature.....

Co-advisor's signature.....

Acknowledgements

I am greatly indebted to Assistant Professor Dr. Pornchai Satravaha, my thesis advisor, for his untiring offering me some thoughtful and helpful advice. I can say that this thesis will not be successful without him. I would also like to thank Associate Professor Suchada Siripant and Associate Professor Dr. Jack Asavanant, my thesis committee, for their suggestions to this thesis. I wish to express my thanks to Professor Songping Zhu for pointing out this problem to me, and to Professor Peter Tritscher for giving me a lot of data and useful information. For all of the teachers who have taught me, I would like to thank them for their valuable knowledge. I am also grateful to DPST (Development and Promotion for Science and Technology talent project of Thailand) for providing me financial support. Thanks to all of my friends for giving me happiness. In particular, I would like to express my great gratitude to my family for their love and encouragement during my study.



สถาบันวิทยบริการ
จุฬาลงกรณ์มหาวิทยาลัย

Contents

1	Introduction	1
2	Mullins equation	4
3	Numerical solution to linear Mullins equation	9
3.1	Cubic splines method	9
3.2	Finite difference method	17
3.3	Laplace transform finite difference method (LTFDM)	20
3.4	Comparison	23
4	Numerical solution to non-linear Mullins equation	25
4.1	Cubic splines method	25
4.2	Finite difference method	36
4.3	Laplace transform finite difference method (LTFDM)	42
4.4	Comparison	57
5	Conclusion	63
	References	66
A	Exact solution for linear Mullins equation	68
B	B_splines	74
C	FDM formula	77
D	Numerical inversion of Laplace transforms	78

Chapter 1

Introduction

Mullins equation is the fourth-order non-linear partial differential equation (PDE) whose solution models the evolution of a surface under the influence of mass transport mechanisms. Herein, the Mullins equation describing grain boundary grooving, in which surface diffusion is treated as the dominant mechanism, over another principal mass transport mechanism, evaporation-condensation, is studied.

Mullins [1] considered the surface groove for a material with isotropic properties in the theory of thermal grooving. In order to solve the surface-diffusion problem, he assumed the surface slope to be small, much less than unity, everywhere so that he could linearize his non-linear PDE. Mullins solved the linearized equation analytically to obtain the so-called “small-slope approximation”, which is valid for nearly flat surfaces. Mullins also suggested that for grain boundary grooving the PDE could be transformed to an ordinary differential equation (ODE).

Robertson [2] performed a transformation as indicated by Mullins. The resulting

differential equation is then numerically integrated. The detailed groove shapes are presented for the groove root slope m ranging from 0 to 4. The groove width is within five percent of the small-slope width for all groove root slopes calculated. The groove depth departs by more than ten percent from the small-slope depth for groove root slopes greater than about 0.7.

Zhang and Schneibel [3] used a method of lines approach to solve Mullins equation. It first converted the PDE to a system of ODE's in time space through spatial discretization and then integrated in time by a stiff ODE solver. The numerical results showed excellent agreement with Mullins' analytical "small slope" solution. However, when the groove root slopes are greater than 0.5, differences between Zhang and Schneibel's solution and Mullins' solution develop.

Although no analytic solutions were known for Mullins equation [4], Tritscher and Broadbridge [5] gave the first analytically solvable model in which the governing equation was an alternative modified form of Mullins equation. A solution is achieved by partitioning the surface into subintervals delimited by lines of constant slope. Their model does not rely on the linear or small-slope approximation in which nonlinearity is neglected. Tritscher and Broadbridge's solution therefore provides a based line against which to check other numerical results.

Lee [6] investigated into solving Mullins equation by the finite difference method (FDM). In this case both temporal and spatial derivatives are replaced by finite difference approximation. The accuracy for small slope ($m < 0.5$) is very good. However, error is obviously increased as the value of m is getting larger.

Recently, Mullins equation was solved by Liu [7] using cubic splines to approximate the function of the surface profile. This causes the governing equation being transformed into a system of ODE's which is then solved by a stiff ODE solver. The numerical solution for small slope ($m \leq 0.1$) is in good agreement with the analytical solution. However, when the groove slope is equal to 1, the shape of the profile is still correct but the accuracy is not good enough. Moreover, when the groove slope is more than 1, the program even does not converge [7].

In this thesis we consider the hybrid application of the Laplace transform technique and the finite difference method, called the Laplace transform finite difference method (LTFDM), for solving Mullins equation. This method was used by Chen and co-worker [9] in transient heat conduction problems. The advantage of this method is that the time derivative from the governing differential equation is removed by the Laplace transform, thus reduces the governing equation to an ODE. Furthermore, another advantage of the Laplace transform technique is that it can quickly give a solution at any specific time. Later, Chen and Lin [10] used the same method to solve non-linear transient problems. They concluded that the hybrid application of the Laplace transform technique and the finite difference method is reliable. The Laplace transform has also been incorporated with the dual reciprocity method for solving non-linear diffusion equations with considerable success [11].

We will first test the LTFDM with the linear system involving the linearized Mullins equation before applying it to solve the non-linear system. Our solutions will be compared with the previous ones.

Chapter 2

Mullins equation

As a background knowledge, Mullins equation will be derived in this chapter. In the theory of thermal grooving published in 1957, Mullins investigated the development of surface grooves at the grain boundaries of a heated polycrystal (see Figure 2.1), in which evaporation-condensation and surface diffusion are the two principal mechanisms for mass transport at a metal surface. Herein we will be interested in the grain boundary grooving by surface diffusion only. In other words, we assume surface diffusion is the only process operating. Let $\mu(K)$ be the increase in chemical potential per atom which is transferred from a point of zero curvature to a point of curvature K on the surface. It can be shown that

$$\mu(K) = K\gamma\Omega$$

where γ is the surface-free energy per unit area and Ω the molecular volume.

Therefore, gradients of chemical potential along the surface will be associated with gradients of curvature. These gradients will produce a drift of surface atoms with an average

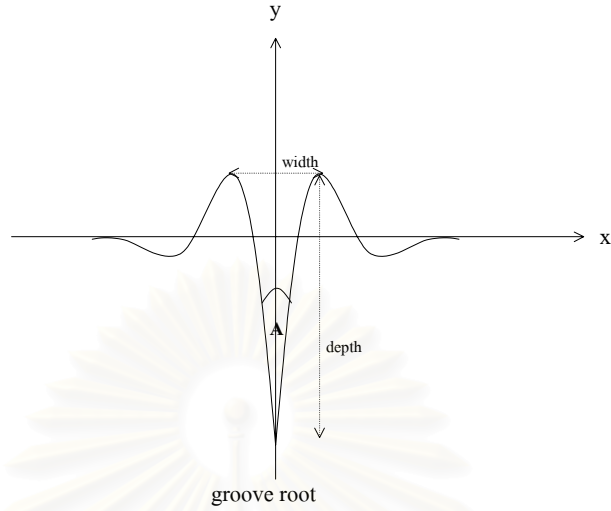


Figure 2.1: A symmetric groove profile.

velocity given by the Nernst-Einstein relation

$$V = -\frac{D_s}{kT} \frac{\partial \mu}{\partial s}$$

where D_s is the coefficient of surface diffusion, s the arc length along the profile, k the Boltzmann constant, and T the absolute temperature. Note that kT is the thermal energy.

The surface flux of atoms, J , is obtained by multiplying V by the number of atoms per unit area or ε . Thus,

$$J = -\frac{D_s \gamma \Omega \varepsilon}{kT} \frac{\partial K}{\partial s};$$

or in term of cartesian coordinates

$$J = -\frac{D_s \gamma \Omega \varepsilon}{kT} (1 + y_x^2)^{-\frac{1}{2}} [y_{xx} (1 + y_x^2)^{-\frac{3}{2}}]_x.$$

The governing equation for the evolution of surface, denoted $y(x, t)$, can be ex-

pressed as

$$y_t = -B\{(1 + y_x^2)^{-\frac{1}{2}}[y_{xx}(1 + y_x^2)^{-\frac{3}{2}}]_x\}_x, \quad (2.1)$$

where $B = D_s\gamma\Omega^2\varepsilon/(kT)$. Equation (2.1) can be written in another form as

$$y_t = -\frac{B}{(1 + y_x^2)^4} [y_{xxxx}(1 + y_x^2)^2 - 10y_x y_{xxx} y_{xxx}(1 + y_x^2) + 3y_{xx}^3(5y_x^2 - 1)],$$

by taking differentiation. The above equation will be referred to as Mullins equation hereafter. In Mullins equation the subscripts x and t of y indicate differentiation with respect to space and time respectively. Equation (2.1) is driven by gradients in surface curvature (K).

As in [1] we impose the boundary condition of zero flux at the groove root. We also impose a fixed dihedral angle A (see Figure 2.1) at the groove root and an initially flat surface. We consider the symmetric grooving case as shown in Figure 2.1. In our numerical calculation we select a sufficiently long interval of x , $[0, L]$, so that the effect of its end $x = L$ on the groove profile is insignificant for the time interval concerned. Here, we set $L = 1$ [7]. The boundary conditions we impose at $x = L$ are zero slope of the surface and zero flux. The first condition corresponds to the initially flat surface. The second condition guarantees the conservation of matter, i.e. a constant area under the groove profile during the evolution.

The governing equation, initial condition, and boundary conditions are as follows:

$$y_t = -\frac{B}{(1 + y_x^2)^4} [y_{xxxx}(1 + y_x^2)^2 - 10y_x y_{xxx} y_{xxx}(1 + y_x^2) + 3y_{xx}^3(5y_x^2 - 1)]; \quad (2.2)$$

subject to

$$\begin{aligned}
\text{IC.} \quad & y(x, 0) = 0, \quad 0 \leq x \leq 1 \\
\text{BC.} \quad & y_x(0, t) = m, \\
& [y_{xxx}(1 + y_x^2) - 3y_x y_{xx}^2]_{x=0} = 0, \\
& y_x(1, t) = 0, \\
& [y_{xxx}(1 + y_x^2) - 3y_x y_{xx}^2]_{x=1} = 0.
\end{aligned} \tag{2.3}$$

Here, m is the slope of the surface at the groove root and is related to the dihedral angle A by

$$m = \tan(90^\circ - (A/2)).$$

It should be noticed that the initial condition, $y(x, 0) = 0$, is not consistent with the boundary condition, $y_x(0, t) = m$. That is, a singularity exists at $x = 0$ and $t = 0$. However, Zhang and Schneibel [3] indicated that this does not pose a barrier in solving the system numerically if we choose a proper numerical method.

Now we will assume that the surface slope is small everywhere ($|y_x| \ll 1$). Let $y_x = 0$ everywhere on interval and replace in Equation (2.1) and Equation (2.3).

Therefore, we will obtain the linear Mullins equation, initial condition, and boundary conditions as follows:

$$y_t = -By_{xxxx} \tag{2.4}$$

subject to

$$\begin{aligned}
 \text{IC. } & y(x, 0) = 0 \\
 \text{BC. } & y_x(0, t) = m \\
 & y_{xxx}(0, t) = 0 \\
 & y_x(1, t) = 0 \\
 & y_{xxx}(1, t) = 0.
 \end{aligned} \tag{2.5}$$

Previously, Mullins derived the equation on a semi-infinite interval such that he had to solve the governing equation with only two boundary conditions, i.e., $y_x(0, t) = m$ and $y_{xxx}(0, t) = 0$, and requires that the solution behaves properly at the infinity. This requirement is consistent with our boundary conditions at $x = 1$, i.e., $y_x(1, t) = 0$ and $y_{xxx}(1, t) = 0$. He assumed the solution in form of power series and obtained the recurrence relation for the coefficients through standard technique. However, the first four coefficients need to be computed separately which involves application of Laplace transform and Taylor's theorem. The "small-slope exact solution" is given in Appendix A.

However, Zhang and Schneibel [3] pointed out that Mullins' solution can easily become unstable when evaluated numerically using a computer. This is due to the limited machine precision and the truncation of the infinite series in which Mullins' solution is presented. To avoid such instability, we solve Equation (2.4) in finite domain, i.e., interval $[0, 1]$, subject to initial and boundary conditions in Equation (2.5) to get the exact solution. Detail is given in Appendix A. We will use our linear solution instead of the small-slope solution for comparison with numerical solutions in the next chapter.

Chapter 3

Numerical solution to linear Mullins equation

In this chapter, we will survey numerical methods previously used to solve Mullins equation along with our proposed LTFDM. They will be investigated for linear Mullins equation and their solutions will be compared with analytic solution.

3.1 Cubic splines method

We will follow Liu's derivation, but with some slight modifications. We want to transform the system of Equations (2.4) and (2.5) to another system involving homogeneous boundary conditions. To do so, let $u(x, t) = y(x, t) + f(x)$. Plugging $y(x, t) = u(x, t) - f(x)$ into Equation (2.4) we find that if we want the form of Equation (2.4) to be preserved, $f^{(4)}$ must be equal to zero. For this reason we choose $f(x) = ax^3 + bx^2 + cx + d$ where a, b, c, d are arbitrary constants. All these constants can be determined by forcing $u(x, t)$ to satisfy

homogeneous boundary conditions as follows:

$$u_x(0, t) = y_x(0, t) + f'(0) = m + c = 0,$$

$$u_{xxx}(0, t) = y_{xxx}(0, t) + f'''(0) = 6a = 0,$$

$$u_x(1, t) = y_x(1, t) + f'(1) = 3a + 2b + c = 0,$$

$$u_{xxx}(1, t) = y_{xxx}(1, t) + f'''(1) = 6a = 0,$$

so that $a = 0$, $b = \frac{m}{2}$, and $c = -m$. Since d can be any number, we choose $d = 0$. Therefore,

$$f(x) = \frac{m}{2}x^2 - mx,$$

which is slightly different from what Liu obtained. Now we have the new system to be solved as:

$$u_t = -Bu_{xxxx}$$

subject to

$$\text{IC. } u(x, 0) = \frac{m}{2}x^2 - mx$$

$$\text{BC. } u_x(0, t) = 0,$$

$$u_{xxx}(0, t) = 0,$$

$$u_x(1, t) = 0,$$

$$u_{xxx}(1, t) = 0.$$

By letting $v = u_{xx}$, the above system can be split into two systems. That is

$$u_t = -Bv_{xx} \tag{3.1}$$

subject to

$$\begin{aligned} \text{IC. } u(x, 0) &= \frac{m}{2}x^2 - mx \\ \text{BC. } u_x(0, t) &= 0, \\ u_x(1, t) &= 0, \end{aligned} \tag{3.2}$$

and

$$v = u_{xx} \tag{3.3}$$

subject to

$$\begin{aligned} \text{BC. } v_x(0, t) &= 0, \\ v_x(1, t) &= 0. \end{aligned} \tag{3.4}$$

Using separation of variable, we approximate u and v by the following expansions

$$u(x, t) = \sum_{k=1}^n c_k(t)\phi_k(x), \tag{3.5}$$

and

$$v(x, t) = \sum_{k=1}^n d_k(t)\varphi_k(x), \tag{3.6}$$

where c_k and d_k are undetermined coefficient functions depending only on t while ϕ_k and φ_k are the basis functions depending only on x . From Equations (3.2) and (3.4), u and v have the same boundary conditions so we can use the same basis functions to expand them, i.e., $\phi_k = \varphi_k$. Here, B_splines are chosen to form basis functions since they are twice continuously differentiable, the property of which is needed in Equations (3.1) and (3.3). (See detail of B_splines in Appendix B.) The basis functions must also be chosen to

satisfy the homogeneous boundary conditions. In this case, we need $\phi'_k(0) = \phi'_k(1) = 0$ for $k = 1, 2, \dots, n$. Therefore, we consider

$$\phi_1(x) = B_1(x)$$

$$\phi_2(x) = B_0(x) + B_2(x)$$

$$\phi_k(x) = B_k(x), \quad k = 3, \dots, n-2$$

$$\phi_{n-1}(x) = B_{n-1}(x) + B_{n+1}(x)$$

$$\phi_n(x) = B_n(x).$$

We now discretize the interval $[0, 1]$ with n nodal points such that $0 = x_1 < x_2 < \dots < x_n = 1$ with equally spacing h . Substituting u from Equation (3.5) and v from Equation (3.6) into Equation (3.1), we have in discretized form

$$\sum_{k=1}^n \dot{c}_k(t) \phi_k(x_i) = -B \sum_{k=1}^n d_k(t) \phi_k''(x_i), \quad i = 1, 2, \dots, n \quad (3.7)$$

where dot and prime denote derivative with respect to t and x , respectively. Equation (3.7) can be written in the matrix form as

$$\Phi \mathbf{c}_t = -B \Phi_{xx} \mathbf{d}.$$

Similarly, Equation (3.3) becomes

$$\sum_{k=1}^n d_k(t) \phi_k(x_i) = \sum_{k=1}^n c_k(t) \phi_k''(x_i), \quad i = 1, 2, \dots, n$$

and is written in the matrix form as

$$\Phi \mathbf{d} = \Phi_{xx} \mathbf{c}.$$

Here,

$$\Phi = \begin{bmatrix} 1 & 1/2 & 0 & 0 & 0 & 0 & 0 \\ 1/4 & 1 & 1/4 & 0 & 0 & 0 & 0 \\ 0 & 1/4 & 1 & 1/4 & 0 & 0 & 0 \\ 0 & 0 & \ddots & \ddots & \ddots & 0 & 0 \\ 0 & 0 & 0 & 1/4 & 1 & 1/4 & 0 \\ 0 & 0 & 0 & 0 & 1/4 & 1 & 1/4 \\ 0 & 0 & 0 & 0 & 0 & 1/2 & 1 \end{bmatrix}$$

and

$$\Phi_{xx} = \frac{1}{h^2} \begin{bmatrix} -3 & 3 & 0 & 0 & 0 & 0 & 0 \\ 3/2 & -3 & 3/2 & 0 & 0 & 0 & 0 \\ 0 & 3/2 & -3 & 3/2 & 0 & 0 & 0 \\ 0 & 0 & \ddots & \ddots & \ddots & 0 & 0 \\ 0 & 0 & 0 & 3/2 & -3 & 3/2 & 0 \\ 0 & 0 & 0 & 0 & 3/2 & -3 & 3/2 \\ 0 & 0 & 0 & 0 & 0 & 3 & -3 \end{bmatrix}.$$

Notice that Φ is tridiagonal and strictly diagonally dominant. By Gershgorin's theorem, Φ is invertible. Therefore,

$$\mathbf{c}_t = -B\Phi^{-1}\Phi_{xx}\mathbf{d},$$

$$\mathbf{d} = \Phi^{-1}\Phi_{xx}\mathbf{c},$$

and hence

$$\mathbf{c}_t = -B(\Phi^{-1}\Phi_{xx})^2\mathbf{c}, \quad (3.8)$$

which is a system of first order ODE's.

System (3.8) together with initial condition in Equation (3.2) form an initial value problem, solution of which at time t_j , called $c^{(j)}$, is obtained through the fourth-order Runge-Kutta method. Once we get $c^{(j)}$, we can compute $u(x_i, t_j)$ by

$$u(x_i, t_j) = \sum_{k=1}^n c_k(t_j) \phi_k(x_i),$$

and our approximate solution is then

$$y_{\text{approx}}(x_i, t_j) = u(x_i, t_j) - mx_i \left(\frac{1}{2} x_i - 1 \right).$$

Figure 3.1 shows numerical solution compared to the exact solution of linear Mullins equation from Appendix A, for groove profile when constant $B = 0.00001$ and slope at the groove root $m = 0.1$ at $t = 1$ using 2000 time steps and 41 nodal points. It can be seen that they are in very good agreement. While we simulated the numerical solutions for several values of m we found that the solution for any value of m is just m multiple of the solution for $m = 1$ or m/r multiple of the solution for $m = r$. This is in accord with the exact solution in which m is the multiplication factor. For this reason we only show the comparison between numerical solution and analytic solution when $m = 0.1$. This means that for any value of m , numerical solution produces groove profile which agrees well with that produced by exact solution.

In the previous work on cubic splines, Liu [7] transformed by using

$$f(x) = \frac{m}{2}(1-x)^2$$

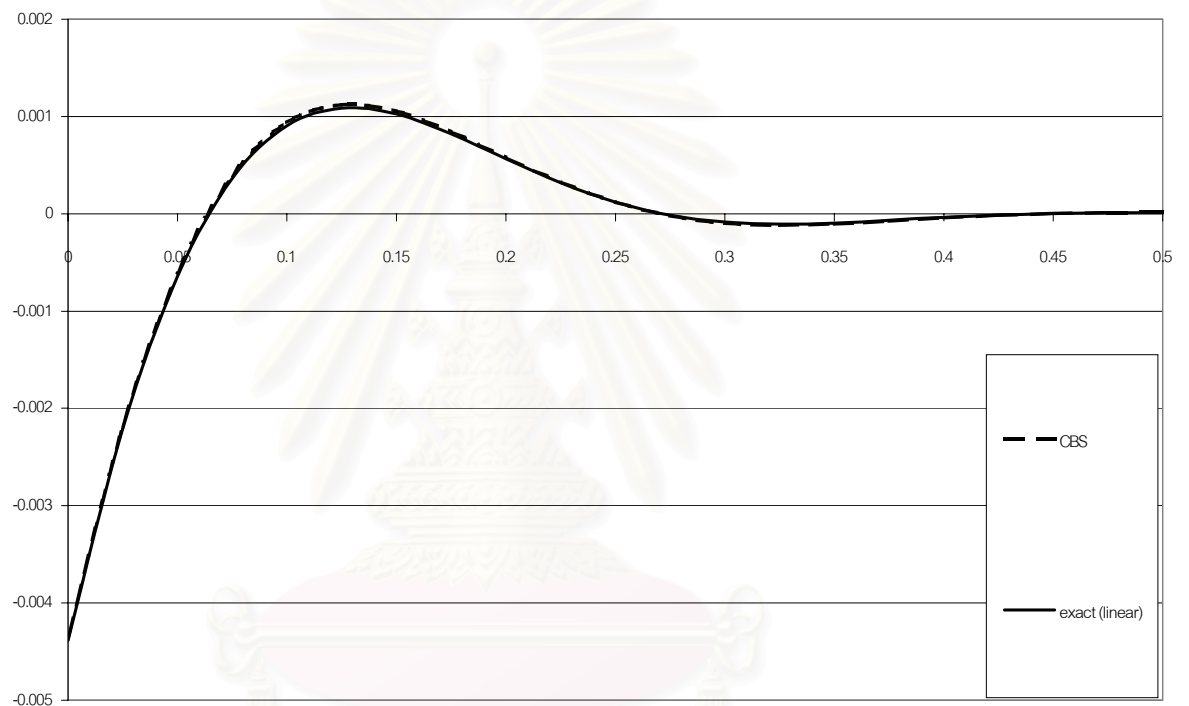


Figure 3.1: Comparison of groove profiles obtained from cubic splines method (dashed line) and analytic solution (solid line) for $m = 0.1$.

จุฬาลงกรณ์มหาวิทยาลัย

and chose ϕ_2 and ϕ_{n-1} differently and they are

$$\phi_2(x) = B_0(x) + B_1(x) + B_2(x),$$

$$\phi_{n-1}(x) = B_{n-1}(x) + B_n(x) + B_{n+1}(x).$$

Then, Φ and Φ_{xx} become

$$\Phi = \begin{bmatrix} 1 & 3/2 & 0 & 0 & 0 & 0 & 0 \\ 1/4 & 5/4 & 1/4 & 0 & 0 & 0 & 0 \\ 0 & 1/4 & 1 & 1/4 & 0 & 0 & 0 \\ 0 & 0 & \ddots & \ddots & \ddots & 0 & 0 \\ 0 & 0 & 0 & 1/4 & 1 & 1/4 & 0 \\ 0 & 0 & 0 & 0 & 1/4 & 5/4 & 1/4 \\ 0 & 0 & 0 & 0 & 0 & 3/2 & 1 \end{bmatrix}$$

and

$$\Phi_{xx} = \frac{1}{h^2} \begin{bmatrix} -3 & 0 & 0 & 0 & 0 & 0 & 0 \\ 3/2 & -3/2 & 3/2 & 0 & 0 & 0 & 0 \\ 0 & 3/2 & -3 & 3/2 & 0 & 0 & 0 \\ 0 & 0 & \ddots & \ddots & \ddots & 0 & 0 \\ 0 & 0 & 0 & 3/2 & -3 & 3/2 & 0 \\ 0 & 0 & 0 & 0 & 3/2 & -3/2 & 3/2 \\ 0 & 0 & 0 & 0 & 0 & 0 & -3 \end{bmatrix}.$$

Notice that now Φ is not strictly diagonally dominant, so it is not guaranteed by Gershgorin's theorem that Φ is nonsingular. However, the result in this case is the same as the one shown in Figure 3.1.

3.2 Finite difference method

Following Lee [6], the interval $[0, 1]$ is equally discretized into $n - 1$ subintervals such that the distance of each subinterval is Δx . The nodal points $i = 1$ and $i = n$ refer to the boundary point 0 and 1 respectively. Moreover, the time t will be discretized into $m - 1$ subintervals, and the distance of each subinterval is Δt (see Figure 3.2).

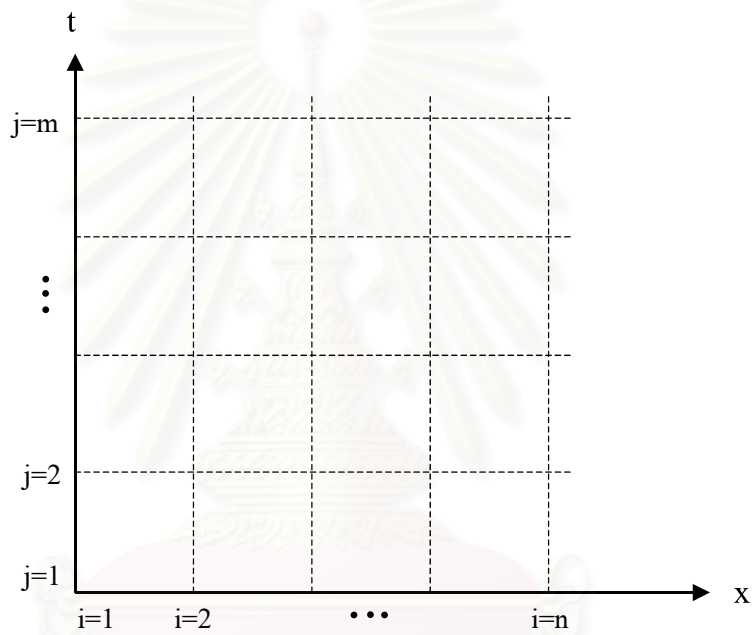


Figure 3.2: The finite difference discretization.

Then, applying the finite difference formulae from Appendix C to approximate Equation (2.4) yields

$$\frac{y_i^{(j+1)} - y_i^{(j)}}{\Delta t} = -B \frac{y_{i+2}^{(j)} - 4y_{i+1}^{(j)} + 6y_i^{(j)} - 4y_{i-1}^{(j)} + y_{i-2}^{(j)}}{\Delta x^4},$$

or, after rearrangement,

$$y_i^{(j+1)} = y_i^{(j)} - \Delta t B \frac{y_{i+2}^{(j)} - 4y_{i+1}^{(j)} + 6y_i^{(j)} - 4y_{i-1}^{(j)} + y_{i-2}^{(j)}}{\Delta x^4}. \quad (3.9)$$

However, doing this leads us into trouble of having points outside $[0, 1]$ involved in the calculation. We can circumvent this problem by applying finite difference formulae to the boundary conditions, thus obtains

$$y_0 = y_2 - 2m \Delta x$$

$$y_{n+1} = y_{n-1}$$

$$y_{-1} = y_3 - 4m \Delta x \quad (3.10)$$

$$y_{n+2} = y_{n-2}.$$

Using Equation (3.9) and (3.10) together with initial condition in Equation (2.5), we can solve the solution at each time step by Jacobi iterative technique. The result for small slope ($m = 0.1$) at $t = 1$ is shown in Figure 3.3 with $B = 0.00001$, 300 time steps, and 41 nodal points being used. Also presented in Figure 3.3 is the graph of exact solution. Obviously, numerical and analytical solutions are in very good agreement.

สถาบันวิทยบริการ
จุฬาลงกรณ์มหาวิทยาลัย

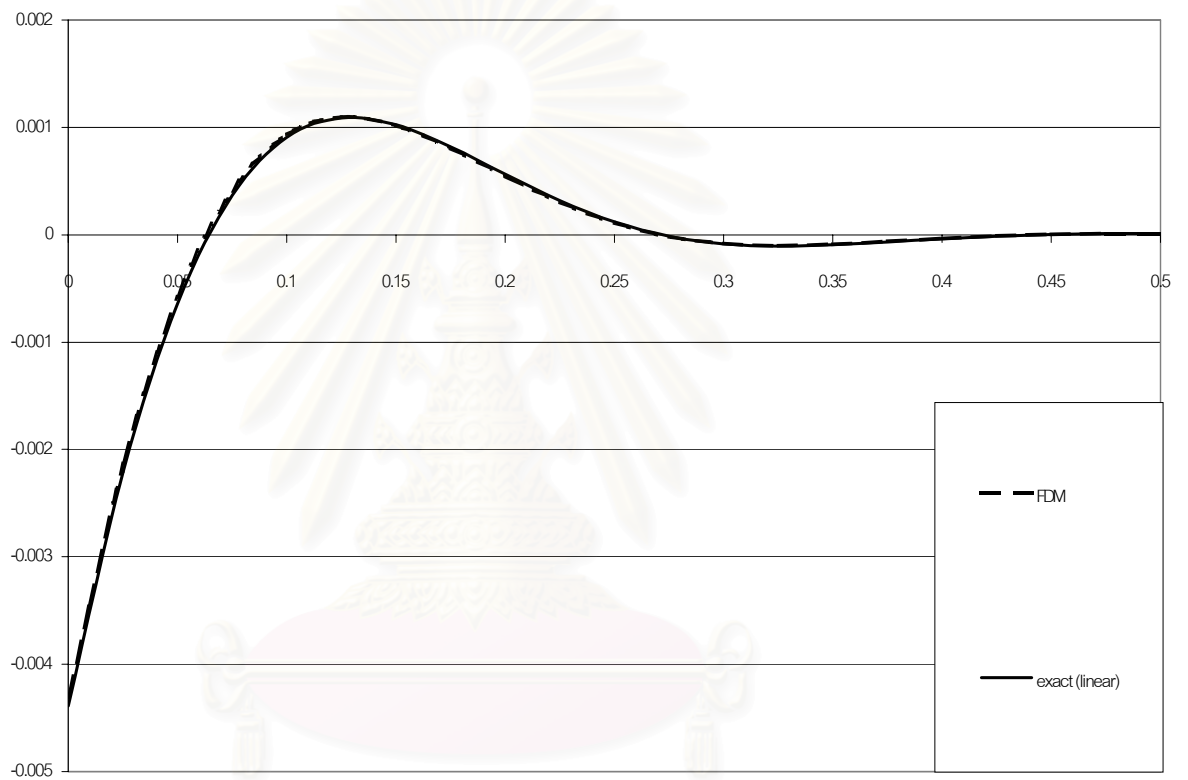


Figure 3.3: Comparison of groove profiles obtained from finite difference method (dashed line) and analytic solution (solid line) for $m = 0.1$.

3.3 Laplace transform finite difference method (LTFDM)

In this section, Mullins equation will be solved by the Laplace transform technique applied in conjunction with the finite difference method. This technique was used, for example, by Chen and Lin [10] in solving one-dimensional transient problems with non-linear material properties.

First, the interval $[0, 1]$ is evenly discretized into $n - 1$ subintervals such that the distance of each subinterval is h . In addition, the nodal points $i = 1$ and $i = n$ refer to the boundary points 0 and 1 respectively as illustrated in Figure 3.4.



Figure 3.4: Diagram of discretization along x-axis.

The approximated form of Equation (2.4), using the central finite difference approximation with the spatial derivative, can be stated as

$$\frac{\partial y_i}{\partial t} = -B \left(\frac{y_{i+2} - 4y_{i+1} + 6y_i - 4y_{i-1} + y_{i-2}}{h^4} \right) \quad (3.11)$$

for $i = 1, 2, \dots, n$, where $y_i = y(x_i, t)$. Taking the Laplace transform of Equation (3.11) with respect to time yields

$$s\hat{y}_i - y(x_i, 0) = -\frac{B}{h^4} \left(\hat{y}_{i+2} - 4\hat{y}_{i+1} + 6\hat{y}_i - 4\hat{y}_{i-1} + \hat{y}_{i-2} \right), \quad (3.12)$$

in which $\hat{y}_i = \hat{y}(x_i, s)$ is the Laplace transform of y_i and s is the Laplace parameter. Equation

(3.12) can be rearranged as

$$\left(\frac{B}{h^4}\right)\hat{y}_{i-2} + \left(-\frac{4B}{h^4}\right)\hat{y}_{i-1} + \left(\frac{6B}{h^4} + s\right)\hat{y}_i + \left(-\frac{4B}{h^4}\right)\hat{y}_{i+1} + \left(\frac{B}{h^4}\right)\hat{y}_{i+2} = y(x_i, 0). \quad (3.13)$$

It should be noted that when $i = 1$, $i = 2$, $i = n-1$, and $i = n$, Equation (3.13) will involve points external to interval $[0, 1]$ as in Section 3.2. However, after applying the finite difference formulae to the boundary conditions in Equation (2.5), the values at external nodes can be computed as follows:

$$\begin{aligned} y_0 &= y_2 - 2mh, \\ y_{n+1} &= y_{n-1}, \\ y_{-1} &= y_3 - 4mh, \\ y_{n+2} &= y_{n-2}. \end{aligned} \quad (3.14)$$

Then taking the Laplace transform of Equation (3.14) with respect to time gives

$$\begin{aligned} \hat{y}_0 &= \hat{y}_2 - \frac{2mh}{s}, \\ \hat{y}_{n+1} &= \hat{y}_{n-1}, \\ \hat{y}_{-1} &= \hat{y}_3 - \frac{4mh}{s}, \\ \hat{y}_{n+2} &= \hat{y}_{n-2}. \end{aligned} \quad (3.15)$$

Equations (3.13) and (3.15) can be rearranged into the matrix form

$$\mathbf{A}\hat{\mathbf{y}} = \mathbf{b} \quad (3.16)$$

where \mathbf{A} is an $(n \times n)$ band matrix, $\hat{\mathbf{y}}$ an $(n \times 1)$ vector representing the unknown \hat{y}_i , and \mathbf{b} an $(n \times 1)$ known constant vector.

Before solving the system (3.16), we need to specify the time t we want solution to be computed. Then we calculate 6 values of s as indicated in the Stehfest's algorithm for numerical inversion of Laplace transform given in Appendix D. Each value of s gives system (3.16) a solution vector $\hat{\mathbf{y}}$. After having solved system (3.16) to get 6 vectors of $\hat{\mathbf{y}}$, the Stehfest's algorithm is utilized to obtain the value of y_i at the specified time.

Depicted in Figure 3.5 are groove profiles obtained from numerical solution by LTFDM and analytical solution for slope $m = 0.1$ at $t = 1$ with $B = 0.00001$ and 41 nodal points being used. Numerical solution is seen to be in excellent agreement with the analytical solution.

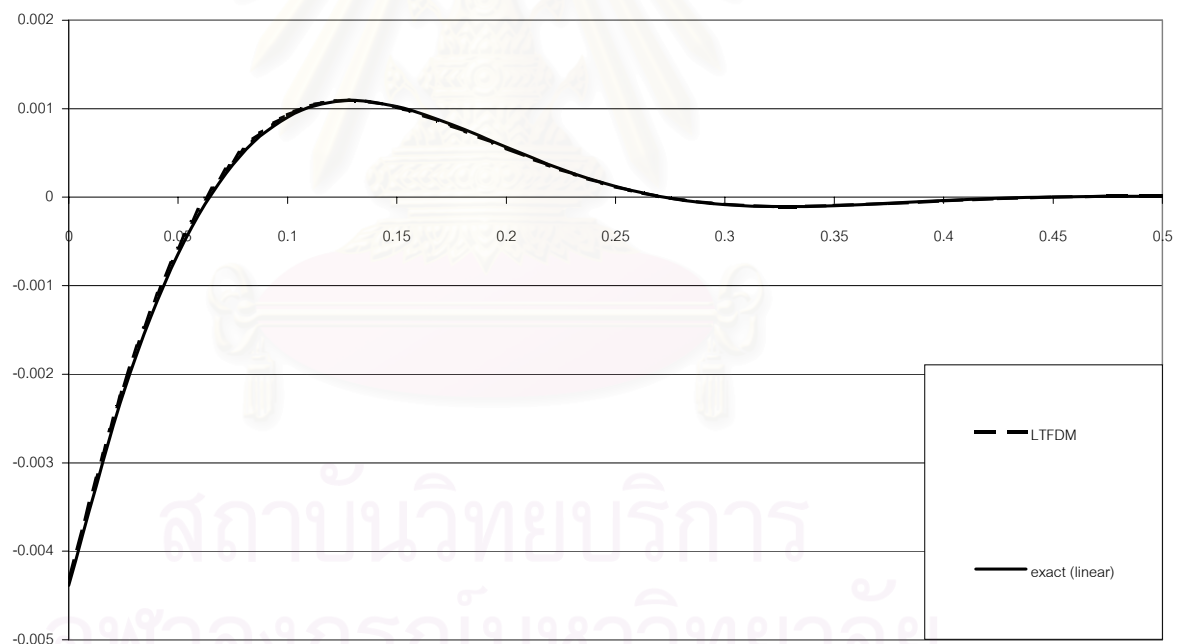


Figure 3.5: Comparison of groove profiles obtained from Laplace transform finite difference method (dashed line) and analytic solution (solid line) for $m = 0.1$.

3.4 Comparison

Now we will compare the results among cubic splines method, FDM, and LTFDM. In Figure 3.6, we see that all methods give similar results which agree very well with the analytic solution. However, the time used for running program in each method is very different when we fix the number of nodes. LTFDM uses time much less than the others. For specific time t , unlike the other two methods which need step-by-step calculations, LTFDM needs only 6 calculations in Laplace space before the numerical inversion is used to retrieve the desired solution. Moreover, if we want to increase the number of nodes for more accuracy, it can be done easily with LTFDM. For cubic splines and finite difference methods, we have to increase the number of time steps when increasing the number of nodes. For example, the stability requirement for FDM is $\frac{B\Delta t}{\Delta x^4} < 0.125$ by the Von Neumann method. In Figure 3.3, the converged solution can still be obtained using 40 subintervals and 300 time steps since $\Delta x = 1/40 = 0.025$, $\Delta t = 1/300$ and $\frac{B\Delta t}{\Delta x^4} = 0.085 < 0.125$, but when increasing the number of subintervals to be 50 ($\Delta x = 0.02$), the solution does not converge with the same number of time steps because $\frac{B\Delta t}{\Delta x^4} = 0.208 \not< 0.125$. Therefore, we have to decrease Δt in order to obtain the solution. Thus, the time used for solution calculation by cubic splines and finite difference methods is much more than that by LTFDM.

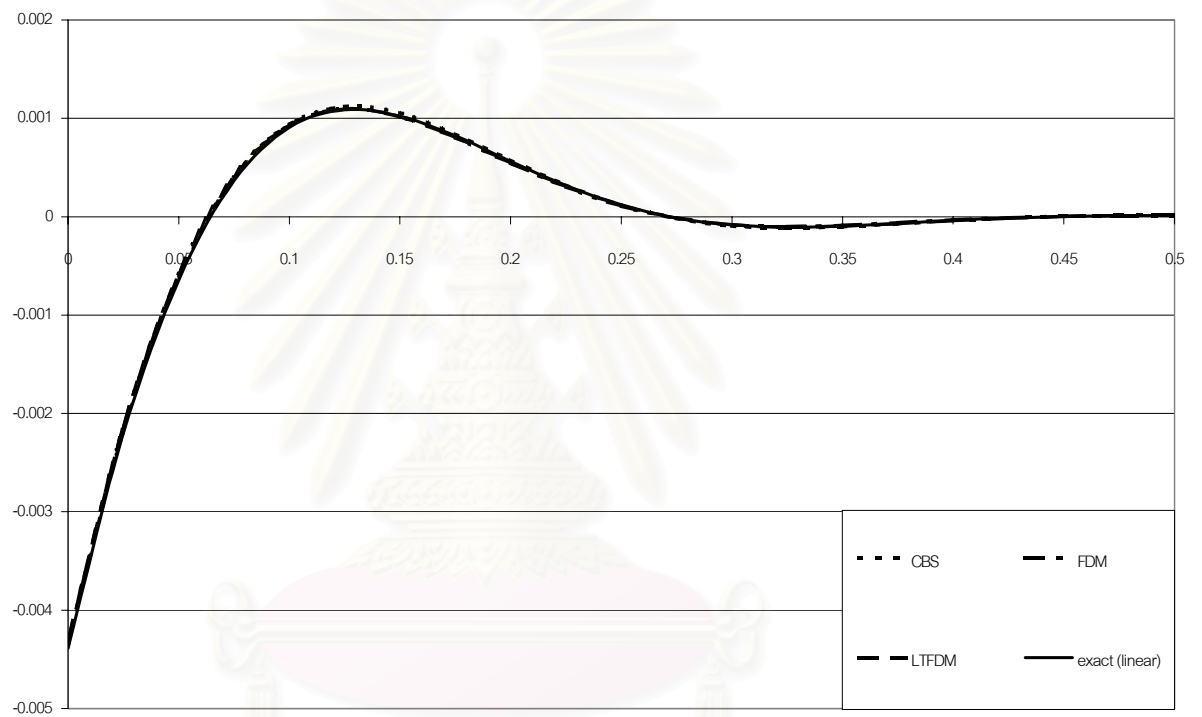


Figure 3.6: Comparison of numerical and analytical solutions for linear Mullins equation when $m = 0.1$.

Chapter 4

Numerical solution to non-linear Mullins equation

In this chapter, we extend the numerical methods surveyed in the previous chapter to non-linear Mullins equation. All numerical results obtained will be compared with that obtained from Tritscher and Broadbridge (T&B)'s analytically solvable model.

4.1 Cubic splines method

Similar to Section 3.1, we transform the system of Equations (2.2) and (2.3) to another one by letting $u(x, t) = y(x, t) + f(x)$ where $f(x) = \frac{m}{2}x^2 - mx$. Hence, we can find

initial condition and boundary conditions in terms of u as

$$\begin{aligned} \text{IC. } u(x, 0) &= \frac{m}{2}x^2 - mx \\ \text{BC. } u_x(0, t) &= 0 \\ u_x(1, t) &= 0 \\ u_{xxx}(0, t) &= \frac{3m(u_{xx}(0, t) - m)^2}{1 + m^2} \\ u_{xxx}(1, t) &= 0. \end{aligned}$$

However, this time we cannot make all the boundary conditions to be homogeneous. Nevertheless, by letting $v = u_{xx}$ the above initial condition and boundary conditions can be separated into two parts, i.e.,

$$\begin{aligned} \text{IC. } u(x, 0) &= \frac{m}{2}x^2 - mx \\ \text{BC. } u_x(0, t) &= 0 \\ u_x(1, t) &= 0 \end{aligned} \tag{4.1}$$

and

$$\begin{aligned} \text{BC. } v_x(0, t) &= \frac{3m(v(0, t) - m)^2}{1 + m^2} \\ v_x(1, t) &= 0. \end{aligned} \tag{4.2}$$

We now discretize the interval $[0, 1]$ with n nodal points such that $0 = x_1 < x_2 < \dots < x_n = 1$ with equally spacing h . Now u and v can be approximated by the following expansion

$$u(x, t) = \sum_{k=1}^n c_k(t) \phi_k(x)$$

and

$$v(x, t) = \sum_{k=1}^n d_k(t) \varphi_k(x).$$

As before, ϕ_k and φ_k are the basis functions chosen so as to satisfy homogeneous boundary conditions. It should be noted that boundary conditions in Equations (4.1) and (4.2) are not the same, so we can not immediately use $\phi_k = \varphi_k$.

From boundary conditions in Equation (4.1), we require that $\phi'_k(0) = \phi'_k(1) = 0$ for $k = 1, 2, \dots, n$. Therefore, we select

$$\phi_1(x) = B_1(x)$$

$$\phi_2(x) = B_0(x) + B_2(x)$$

$$\phi_k(x) = B_k(x), \quad k = 3, \dots, n-2$$

$$\phi_{n-1}(x) = B_{n-1}(x) + B_{n+1}(x)$$

$$\phi_n(x) = B_n(x),$$

which satisfy the requirement.

On the other hand, φ_k must be chosen to satisfy boundary conditions for v in Equation (4.2). Thus, we need $\varphi'_k(1) = 0$ but $\varphi'_k(0)$ is not necessary to be zero, for $k = 1, 2, \dots, n$. Let us consider the set of $\{\varphi_k\}_{k=1}^n$ to be the same as $\{\phi_k\}_{k=1}^n$ except for φ_2 that we choose

$$\varphi_2(x) = B_2(x).$$

It is obvious that, by taking differentiation, we have $\varphi'_k(0) = 0$ for $k = 1, 3, 4, \dots, n$ and $\varphi'_k(1) = 0$ for $k = 1, 2, 3, \dots, n$, and

$$\varphi'_2(0) = B'_2(0) = \frac{3}{4h}.$$

Since $v_x(0, t) = \frac{3m(v(0, t) - m)^2}{1 + m^2}$ and

$$\begin{aligned} v_x(0, t) &= \sum_{k=1}^n d_k(t) \varphi'_k(0) \\ &= d_1(t) \varphi'_1(0) + d_2(t) \varphi'_2(0) + d_3(t) \varphi'_3(0) + \cdots + d_n(t) \varphi'_n(0) \\ &= \frac{3}{4h} d_2(t) \end{aligned}$$

and

$$\begin{aligned} v(0, t) &= u_{xx}(0, t) = \sum_{k=1}^n c_k(t) \phi''_k(0) \\ &= c_1(t) \phi''_1(0) + c_2(t) \phi''_2(0) + c_3(t) \phi''_3(0) + \cdots + c_n(t) \phi''_n(0) \\ &= c_1(t) B''_1(0) + c_2(t) [B''_0(0) + B''_2(0)] + c_3(t) B''_3(0) + \cdots + c_n(t) B''_n(0) \\ &= c_1(t) \left(-\frac{3}{h^2} \right) + c_2(t) \left(\frac{3}{2h^2} + \frac{3}{2h^2} \right) + c_3(t) \cdot 0 + \cdots + c_n(t) \cdot 0 \\ &= \frac{3}{h^2} [c_2(t) - c_1(t)], \end{aligned}$$

we finally have

$$\frac{3}{4h} d_2(t) = \frac{3m}{1 + m^2} \left\{ \frac{3}{h^2} [c_2(t) - c_1(t)] - m \right\}^2,$$

and hence

$$d_2(t) = \frac{4mh}{1 + m^2} \left\{ \frac{3}{h^2} [c_2(t) - c_1(t)] - m \right\}^2.$$

Now we write v in terms of ϕ_k 's as follows:

$$\begin{aligned} v(x, t) &= \sum_{k=1}^n d_k(t) \varphi_k(x) \\ &= d_1(t) B_1(x) + d_2(t) B_2(x) + d_3(t) B_3(x) + \cdots + d_n(t) B_n(x) \\ &= \{d_1(t) B_1(x) + d_2(t) [B_0(x) + B_2(x)] + d_3(t) B_3(x) + \cdots + d_n(t) B_n(x)\} - d_2(t) B_0(x) \\ &= \sum_{k=1}^n d_k(t) \phi_k(x) - \frac{4mh}{1 + m^2} \left\{ \frac{3}{h^2} [c_2(t) - c_1(t)] - m \right\}^2 B_0(x). \end{aligned}$$

From $v = u_{xx}$, we will have

$$\sum_{k=1}^n d_k(t) \phi_k(x) - \frac{4mh}{1+m^2} \left\{ \frac{3}{h^2} [c_2(t) - c_1(t)] - m \right\}^2 B_0(x) = \sum_{k=1}^n c_k(t) \phi_k''(x).$$

Applying this equation to all nodal points yields

$$\mathbf{d} = \Phi^{-1} \Phi_{xx} \mathbf{c} + \Phi^{-1} \mathbf{g} \quad (4.3)$$

where \mathbf{c} , \mathbf{d} , Φ^{-1} , and Φ_{xx} are the same as in Section 3.1, and

$$\mathbf{g} = \begin{bmatrix} \frac{4mh}{1+m^2} \left\{ \frac{3}{h^2} [c_2(t) - c_1(t)] - m \right\}^2 B_0(0) \\ 0 \\ \vdots \\ 0 \end{bmatrix}.$$

Remembering that $y(x, t) = u(x, t) - f(x)$, we have

$$y_t = u_t(x, t) = \sum_{k=1}^n \dot{c}_k(t) \phi_k(x),$$

$$y_x = u_x(x, t) - f'(x) = \sum_{k=1}^n c_k(t) \phi_k'(x) - (mx - m),$$

$$y_{xx} = u_{xx}(x, t) - f''(x) = \sum_{k=1}^n c_k(t) \phi_k''(x) - m,$$

$$y_{xxx} = v_x(x, t) - f'''(x) = \sum_{k=1}^n d_k(t) \phi_k'(x) - \frac{4mh}{1+m^2} \left\{ \frac{3}{h^2} [c_2(t) - c_1(t)] - m \right\}^2 B_0'(x),$$

$$y_{xxxx} = v_{xx}(x, t) - f^{(4)}(x) = \sum_{k=1}^n d_k(t) \phi_k''(x) - \frac{4mh}{1+m^2} \left\{ \frac{3}{h^2} [c_2(t) - c_1(t)] - m \right\}^2 B_0''(x).$$

We now substitute the above 5 derivatives into the original non-linear Mullins equation (2.2) and use Equation (4.3) to compute the coefficient function d_k 's in terms of c_k 's. We finally arrive at a system of n ODE's in matrix form as

$$\Phi \mathbf{c}_t = f(t, \mathbf{c}) \quad (4.4)$$

We can solve system (4.4) using Runge-Kutta-Fehlberg method with

$$\begin{aligned} \mathbf{c}_0 &= \Phi^{-1} \mathbf{u}_0 \\ &= \Phi^{-1} \begin{bmatrix} u(x_1, 0) \\ \vdots \\ u(x_n, 0) \end{bmatrix}. \end{aligned}$$

Then we will get $u(x, t)$ and, finally, $y(x, t)$.

In the previous work, Liu [7] transformed the system of Equation (2.3) by letting $f(x) = \frac{m}{2}(1-x)^2 + \frac{m}{\pi^2} \cos \pi x$, and chose ϕ_2 and ϕ_{n-1} differently which are

$$\begin{aligned} \phi_2(x) &= B_0(x) + B_1(x) + B_2(x), \\ \phi_{n-1}(x) &= B_{n-1}(x) + B_n(x) + B_{n+1}(x). \end{aligned}$$

Additionally, φ_2 and φ_{n-1} were chosen to be

$$\begin{aligned} \varphi_2(x) &= AB_0(x) + B_1(x) + B_2(x), \\ \varphi_{n-1}(x) &= B_{n-1}(x) + B_n(x) + B_{n+1}(x). \end{aligned}$$

where

$$A = 1 - \frac{36m}{(1+m^2)h^3} \frac{c_1^2(t)}{d_2^2(t)}.$$

The solution could be obtained through IMSL ODE package DIVPAG [7], however, we will use Runge-Kutta-Fehlberg method instead. In this case, we find that the result obtained from our derivation is very close to that from Liu's.

Figures 4.1 - 4.5 shows the results using our derivation for $m = 0.1, 0.5, 0.7, 0.8, 1$ at $t = 1$. They are compared with T&B's solution. Our solutions are close to T&B's solutions for the value of m up to 0.5 and they start to depart from T&B's solution when $m > 0.5$. Here, we use 41 nodal points with 2000 time steps for the calculation.

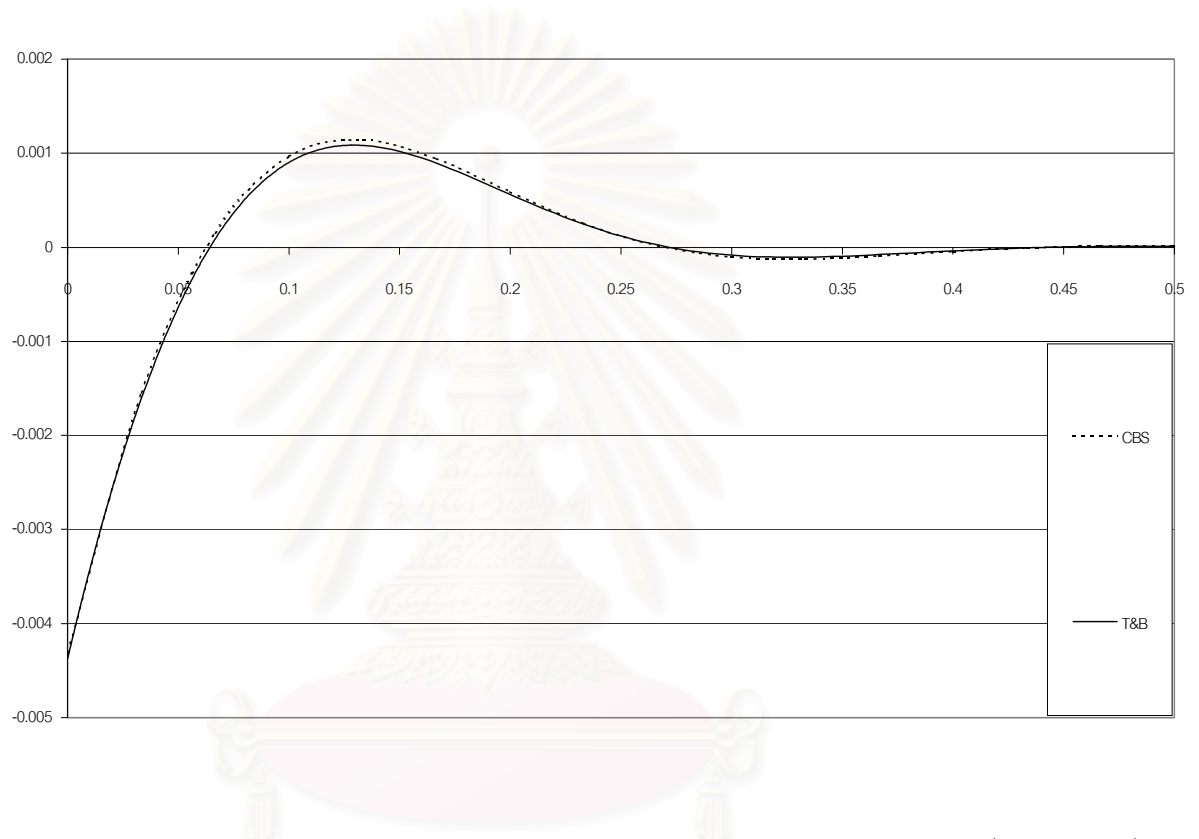


Figure 4.1: Comparison of groove profiles produced from cubic splines method (dotted line) and T&B's solution (solid line) for $m = 0.1$.

สถาบันวิทยบริการ
จุฬาลงกรณ์มหาวิทยาลัย

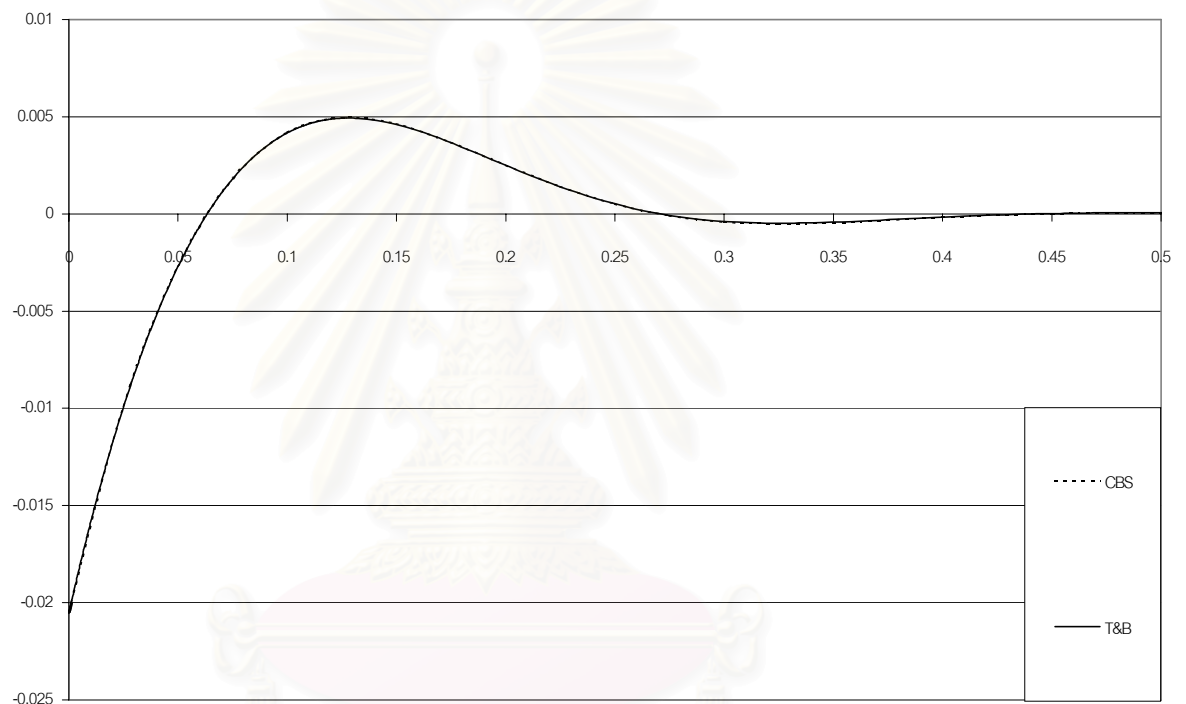


Figure 4.2: Comparison of groove profiles produced from cubic splines method (dotted line) and T&B's solution (solid line) for $m = 0.5$.

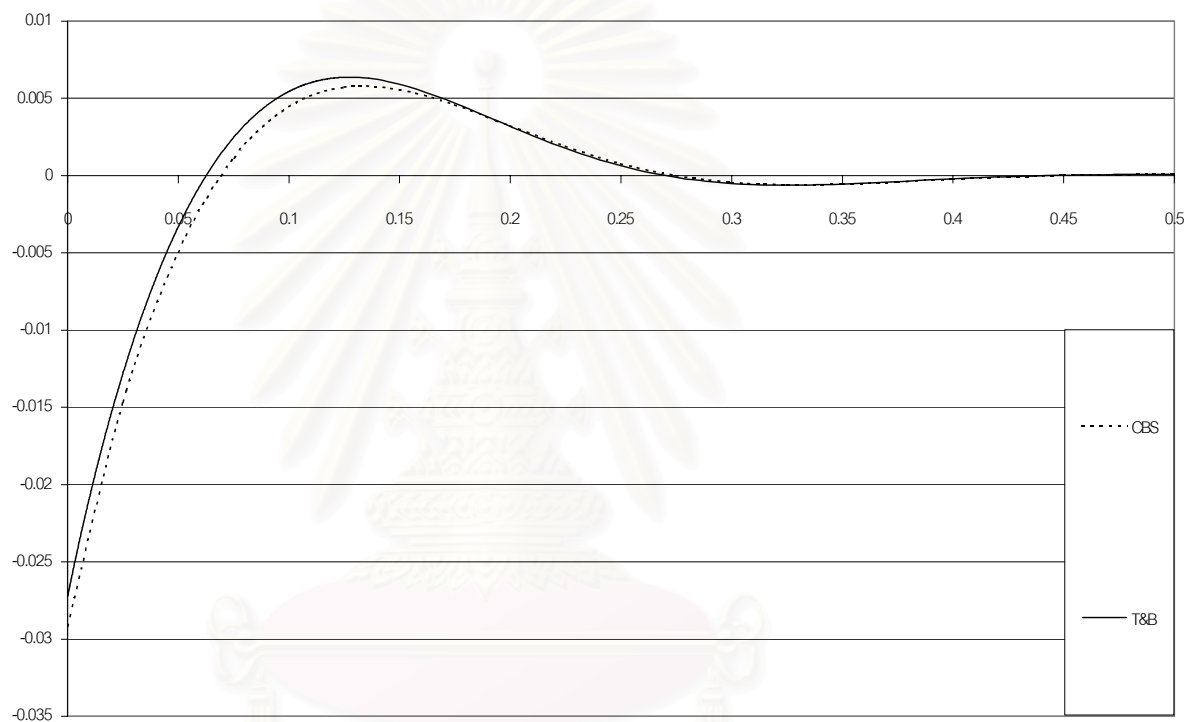


Figure 4.3: Comparison of groove profiles produced from cubic splines method (dotted line) and T&B's solution (solid line) for $m = 0.7$.

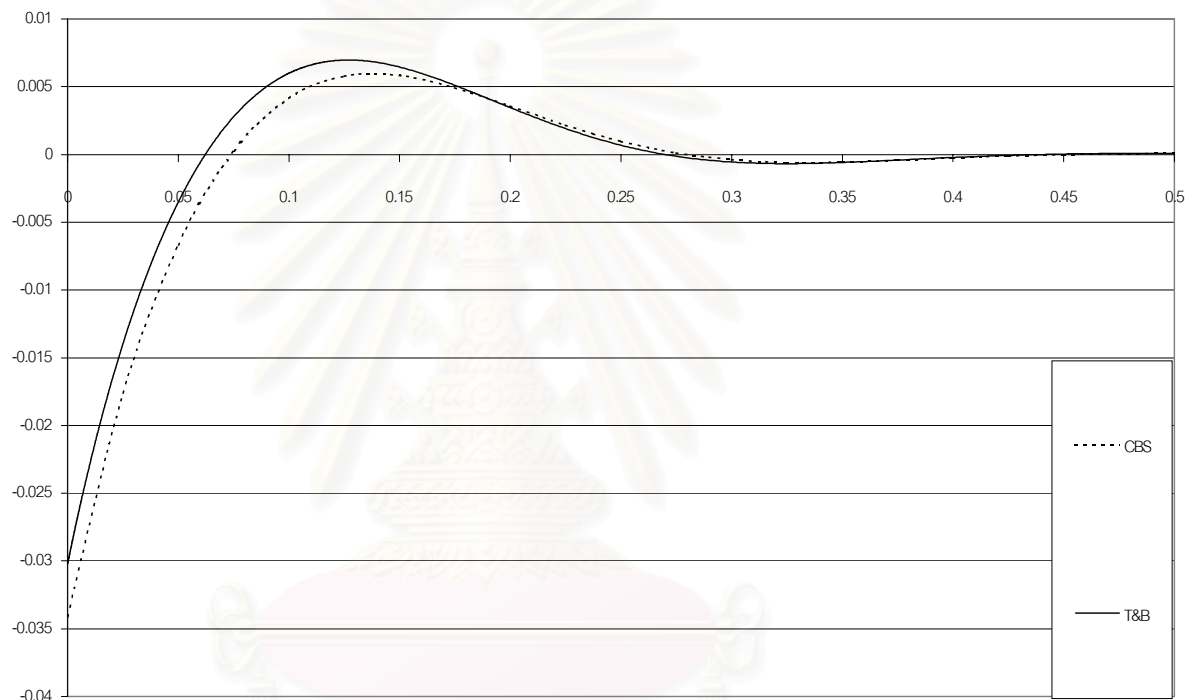


Figure 4.4: Comparison of groove profiles produced from cubic splines method (dotted line) and T&B's solution (solid line) for $m = 0.8$.

จุฬาลงกรณ์มหาวิทยาลัย

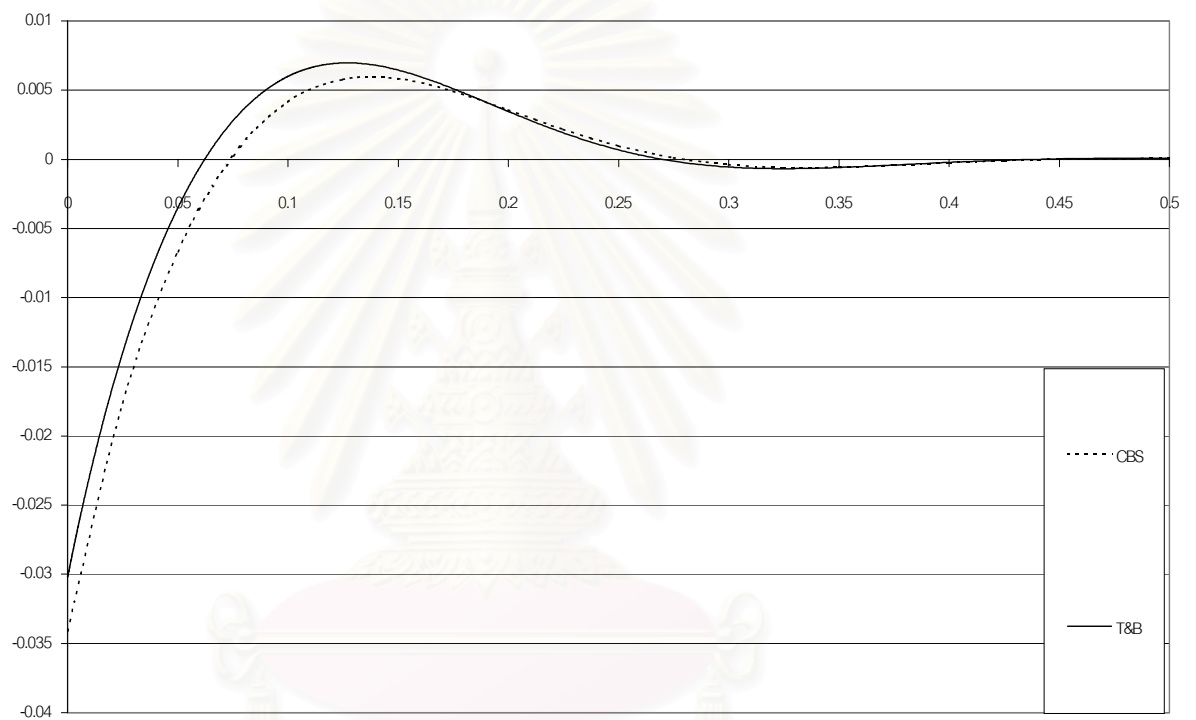


Figure 4.5: Comparison of groove profiles produced from cubic splines method (dotted line) and T&B's solution (solid line) for $m = 1.0$.

จุฬาลงกรณ์มหาวิทยาลัย

4.2 Finite difference method

We use the forward finite difference formula for the first order derivative with y_t in Equation (2.2) yields

$$\frac{y^{(j+1)} - y^{(j)}}{\Delta t} = -\frac{B}{\left(1 + \left(y_x^{(j)}\right)^2\right)^4} \left[y_{xxxx}^{(j)} \left(1 + \left(y_x^{(j)}\right)^2\right)^2 - 10y_x^{(j)} y_{xx}^{(j)} y_{xxx}^{(j)} \left(1 + \left(y_x^{(j)}\right)^2\right) + 3 \left(y_{xx}^{(j)}\right)^3 \left(5 \left(y_x^{(j)}\right)^2 - 1\right) \right],$$

then, after rearrangement,

$$y^{(j+1)} = y^{(j)} - \frac{B \Delta t}{\left(1 + \left(y_x^{(j)}\right)^2\right)^4} \left[y_{xxxx}^{(j)} \left(1 + \left(y_x^{(j)}\right)^2\right)^2 - 10y_x^{(j)} y_{xx}^{(j)} y_{xxx}^{(j)} \left(1 + \left(y_x^{(j)}\right)^2\right) + 3 \left(y_{xx}^{(j)}\right)^3 \left(5 \left(y_x^{(j)}\right)^2 - 1\right) \right]. \quad (4.5)$$

We can approximate y_x , y_{xx} , y_{xxx} , and y_{xxxx} by using the symmetry finite difference formulae from Appendix C. However, we still have problem with the unknown external points. Hence, we have to apply the finite difference formulae with the boundary conditions in Equation (2.3), and we will obtain

$$y_0 = y_2 - 2m \Delta x,$$

$$y_{n+1} = y_{n-1}, \quad (4.6)$$

$$y_{-1} = -\frac{6 \Delta x^3 y_x y_{xx}^2}{1 + y_x^2} + y_3 - 4m \Delta x,$$

$$y_{n+2} = \frac{6 \Delta x^3 y_x y_{xx}^2}{1 + y_x^2} + y_{n-2}.$$

We solve Equations (4.5) and (4.6) together with the initial condition in Equation (2.3) using Jacobi iterative technique. Figures 4.6 and 4.7 display groove profiles produced

by FDM and T&B's solution for $m = 0.1$ and 0.5 . We can see that both graphs in each figure are in very good agreement with each other. However, when we increase the slope at groove root or the values of m to more than 0.5 , the profile produced by FDM starts to depart from that produced by T&B's solution (see Figure 4.8 - 4.10). For $m = 0.1$, the number of nodal points used is 31 with 500 time steps. When increasing the value of m , we have to increase the number of nodal points for more accuracy so that we have to increase the number of time steps also. For $m = 1$, we use 81 nodal points with 4000 time steps in the production of groove profile.

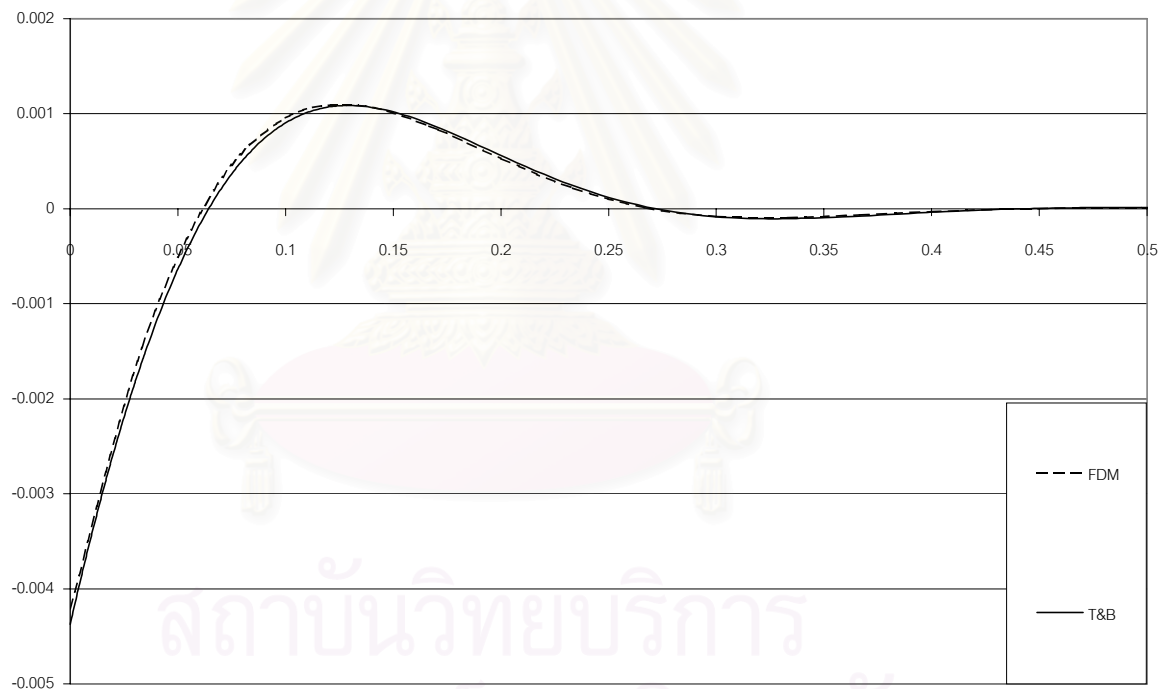


Figure 4.6: Comparison of groove profiles produced from FDM (dashed line) and T&B's solution (solid line) for $m = 0.1$.

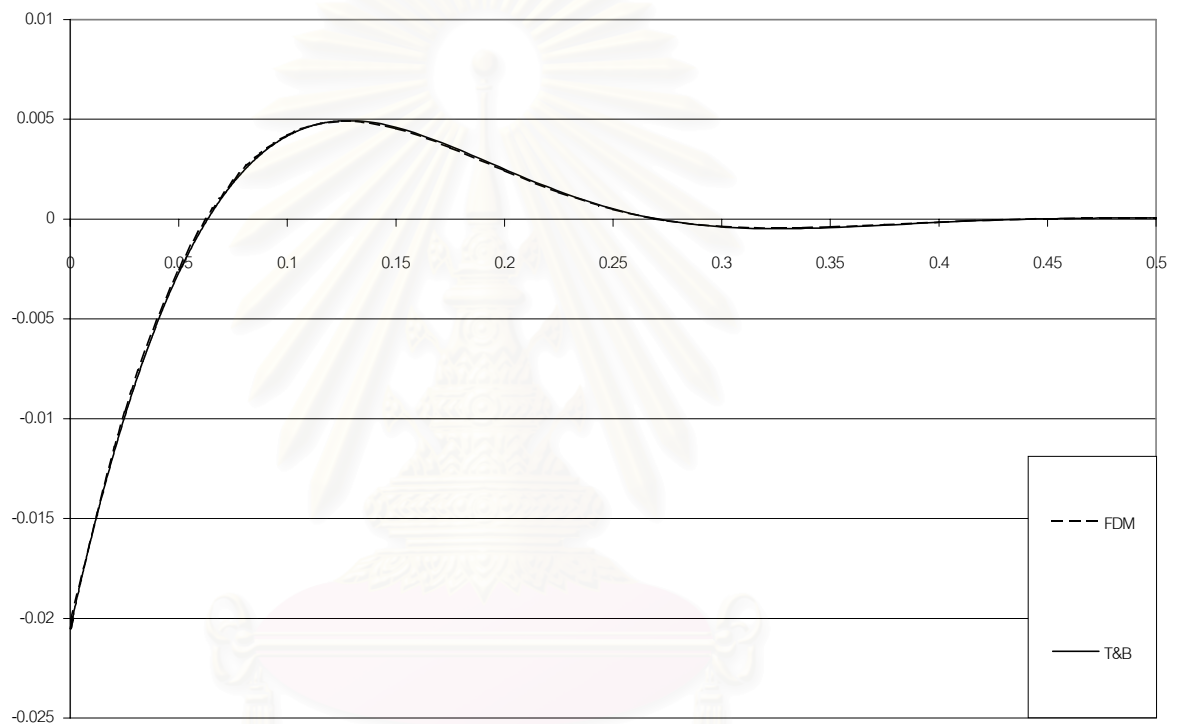


Figure 4.7: Comparison of groove profiles produced from FDM (dashed line) and T&B's solution (solid line) for $m = 0.5$.

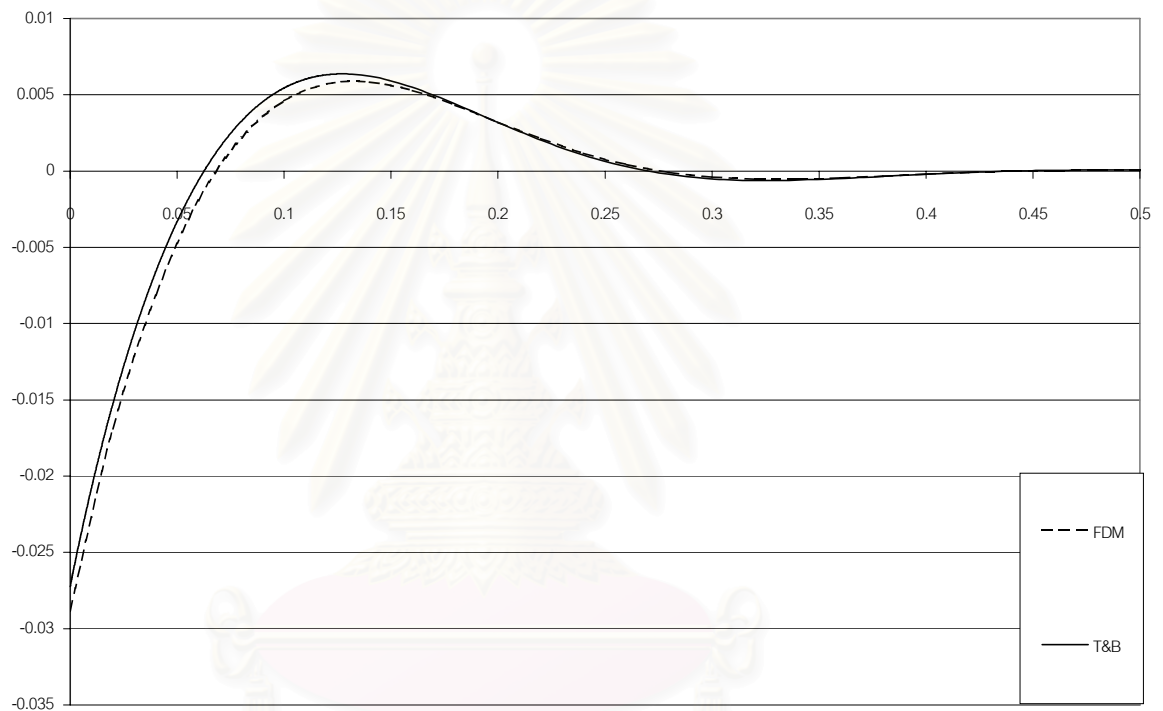


Figure 4.8: Comparison of groove profiles produced from FDM (dashed line) and T&B's solution (solid line) for $m = 0.7$.

จุฬาลงกรณ์มหาวิทยาลัย

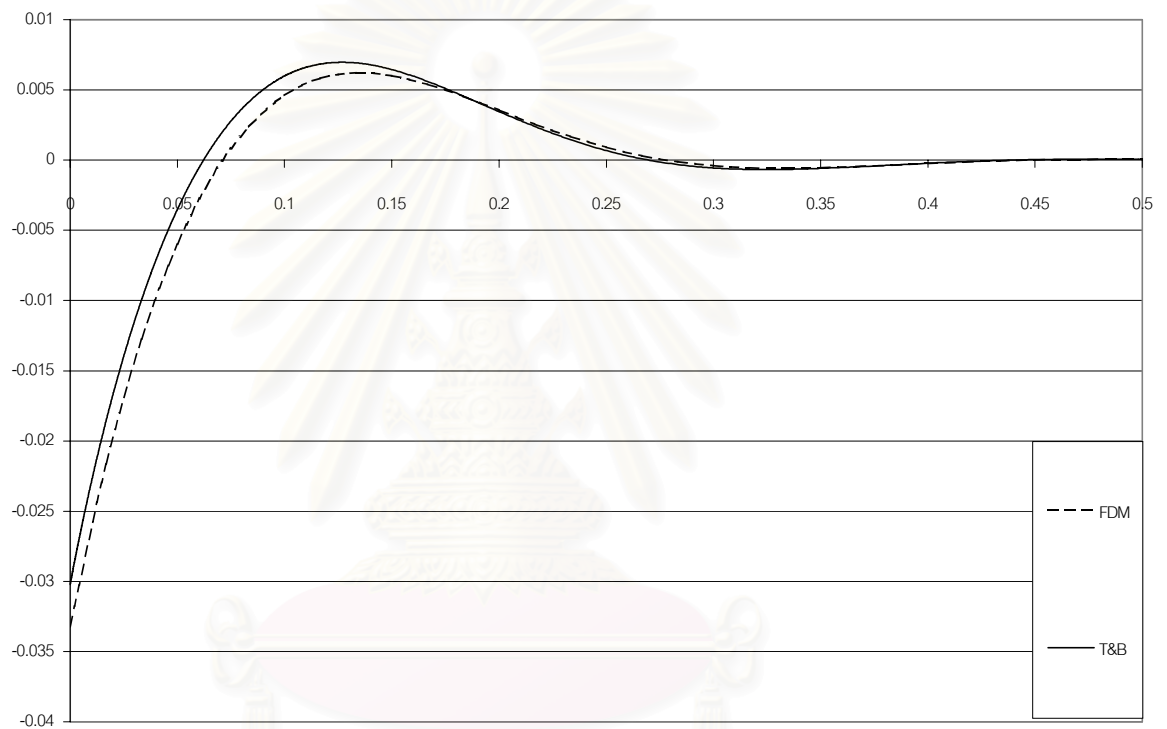


Figure 4.9: Comparison of groove profiles produced from FDM (dashed line) and T&B's solution (solid line) for $m = 0.8$.

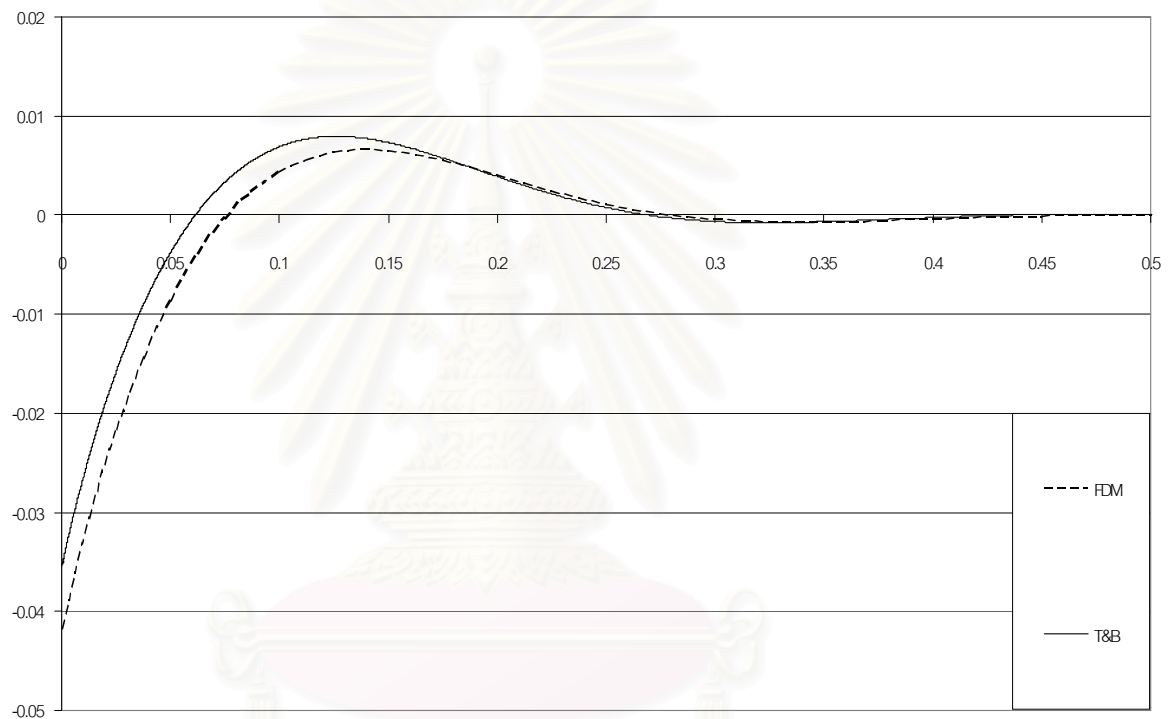


Figure 4.10: Comparison of groove profiles produced from FDM (dashed line) and T&B's solution (solid line) for $m = 1.0$.

จุฬาลงกรณ์มหาวิทยาลัย

4.3 Laplace transform finite difference method (LTFDM)

In order to use LTFDM, unlike the linear Mullins equation which can be solved without any trouble, the non-linear Mullins equation needs linearization to relieve the non-linear structure. That is the non-linear terms must be linearized before applying FDM. The linearized variable will be written with \sim which denotes the previous iteration. In this thesis, we propose two linearization schemes including direct scheme and Taylor series expansion scheme.

Direct linearization scheme

For this scheme, we will keep the highest order spatial derivative terms as many as possible with the rest being written with \sim . Thus, Equation (2.2) can be rewritten as

$$\frac{\partial y}{\partial t} = -\frac{B}{(1 + \tilde{y}_x^2)^4} \left[(1 + \tilde{y}_x^2)^2 \cdot y_{xxxx} - 10\tilde{y}_x \tilde{y}_{xx} (1 + \tilde{y}_x^2) \cdot y_{xxx} + 3(5\tilde{y}_x^2 - 1)\tilde{y}_{xx}^2 \cdot y_{xx} \right]$$

Using the symmetry finite difference formulae from Appendix C to approximate y_{xx} , y_{xxx} , y_{xxxx} yields

$$\begin{aligned} \frac{\partial y_i}{\partial t} = & -\frac{B}{(1 + \tilde{y}_x^2)^4} \left[(1 + \tilde{y}_x^2)^2 \cdot \left(\frac{y_{i+2} - 4y_{i+1} + 6y_i - 4y_{i-1} + y_{i-2}}{h^4} \right) \right. \\ & - 10\tilde{y}_x \tilde{y}_{xx} (1 + \tilde{y}_x^2) \cdot \left(\frac{y_{i+2} - 2y_{i+1} + 2y_{i-1} - y_{i-2}}{2h^3} \right) \\ & \left. + 3(5\tilde{y}_x^2 - 1)\tilde{y}_{xx}^2 \cdot \left(\frac{y_{i+1} - 2y_i + y_{i-1}}{h^2} \right) \right], \end{aligned} \quad (4.7)$$

for $i = 1, 2, \dots, n$. It should be remarked that \tilde{y}_x and \tilde{y}_{xx} are also approximated by the finite difference formulae. However, for conciseness, they will be left as they are in Equation

(4.7). Taking Laplace transform of Equation (4.7) with respect to t , it follows that

$$\begin{aligned}
\hat{sy}_i - y(x_i, 0) = & - \left(\frac{B}{(1 + \tilde{y}_x^2)^4} \right) \left\{ \left[\frac{(1 + \tilde{y}_x^2)^2}{h^4} + \frac{5\tilde{y}_x\tilde{y}_{xx}(1 + \tilde{y}_x^2)}{h^3} \right] \hat{y}_{i-2} \right. \\
& - \left[\frac{4(1 + \tilde{y}_x^2)^2}{h^4} + \frac{10\tilde{y}_x\tilde{y}_{xx}(1 + \tilde{y}_x^2)}{h^3} - \frac{3(5\tilde{y}_x^2 - 1)\tilde{y}_{xx}^2}{h^2} \right] \hat{y}_{i-1} \\
& + \left[\frac{6(1 + \tilde{y}_x^2)^2}{h^4} - \frac{6(5\tilde{y}_x^2 - 1)\tilde{y}_{xx}^2}{h^2} \right] \hat{y}_i \\
& - \left[\frac{4(1 + \tilde{y}_x^2)^2}{h^4} - \frac{10\tilde{y}_x\tilde{y}_{xx}(1 + \tilde{y}_x^2)}{h^3} - \frac{3(5\tilde{y}_x^2 - 1)\tilde{y}_{xx}^2}{h^2} \right] \hat{y}_{i+1} \\
& \left. + \left[\frac{(1 + \tilde{y}_x^2)^2}{h^4} - \frac{5\tilde{y}_x\tilde{y}_{xx}(1 + \tilde{y}_x^2)}{h^3} \right] \hat{y}_{i+2} \right\}
\end{aligned} \tag{4.8}$$

where $i = 1, 2, \dots, n$.

Now we approximate the boundary conditions in Equation (2.3) by finite difference formulae so that two of the boundary conditions are as follows:

$$\begin{aligned}
y_x(0, t) = m & \Rightarrow y_0 = y_2 - 2mh, \\
y_x(1, t) = 0 & \Rightarrow y_{n+1} = y_{n-1}.
\end{aligned}$$

The rest of the boundary conditions must be linearized. We can linearize $y_{xxx}(1 + y_x^2) - 3y_x y_{xx}^2$ to be $(1 + \tilde{y}_x^2)y_{xxx} - 3\tilde{y}_x\tilde{y}_{xx}y_{xx}$. Thus, from $[y_{xxx}(1 + y_x^2) - 3y_x y_{xx}^2]|_{x=0} = 0$ we have

$$(1 + \tilde{y}_x^2) \left[\frac{y_3 - 2y_2 + 2y_0 - y_{-1}}{2h^3} \right] - 3\tilde{y}_x\tilde{y}_{xx} \left[\frac{y_2 - 2y_1 + y_0}{h^2} \right] = 0$$

or

$$y_{-1} = \frac{12h\tilde{y}_x\tilde{y}_{xx}}{1 + \tilde{y}_x^2} \cdot y_1 - \frac{12h\tilde{y}_x\tilde{y}_{xx}}{1 + \tilde{y}_x^2} \cdot y_2 + y_3 + \left[\frac{12mh^2\tilde{y}_x\tilde{y}_{xx}}{1 + \tilde{y}_x^2} - 4mh \right].$$

For $[y_{xxx}(1 + y_x^2) - 3y_x y_{xx}^2]|_{x=1} = 0$, we have

$$(1 + \tilde{y}_x^2) \left[\frac{y_{n+2} - 2y_{n+1} + 2y_{n-1} - y_{n-2}}{2h^3} \right] - 3\tilde{y}_x\tilde{y}_{xx} \left[\frac{y_{n+1} - 2y_n + y_{n-1}}{h^2} \right] = 0$$

or

$$y_{n+2} = y_{n-2} + \frac{12h\tilde{y}_x\tilde{y}_{xx}}{1+\tilde{y}_x} \cdot y_{n-1} - \frac{12h\tilde{y}_x\tilde{y}_{xx}}{1+\tilde{y}_x} \cdot y_n.$$

Taking Laplace transform of y_0 , y_{n+1} , y_{-1} , and y_{n+2} with respect to time yields

$$\begin{aligned} \hat{y}_0 &= \hat{y}_2 - \frac{2mh}{s}, \\ \hat{y}_{n+1} &= \hat{y}_{n-1}, \\ \hat{y}_{-1} &= \frac{12h\tilde{y}_x\tilde{y}_{xx}}{1+\tilde{y}_x} \cdot \hat{y}_1 - \frac{12h\tilde{y}_x\tilde{y}_{xx}}{1+\tilde{y}_x} \cdot \hat{y}_2 + \hat{y}_3 + \left(\frac{1}{s}\right) \left[\frac{12mh^2\tilde{y}_x\tilde{y}_{xx}}{1+\tilde{y}_x} - 4mh \right], \\ \hat{y}_{n+2} &= \hat{y}_{n-2} + \frac{12h\tilde{y}_x\tilde{y}_{xx}}{1+\tilde{y}_x} \cdot \hat{y}_{n-1} - \frac{12h\tilde{y}_x\tilde{y}_{xx}}{1+\tilde{y}_x} \cdot \hat{y}_n. \end{aligned} \quad (4.9)$$

Taylor series expansion linearization scheme

Now we will use Taylor series expansion scheme to linearize the non-linear terms.

The truncated first order Taylor series expansion states that

$$f(u_1, \dots, u_n) = f(\tilde{u}_1, \dots, \tilde{u}_n) + f_{u_1}(\tilde{u}_1, \dots, \tilde{u}_n)(u_1 - \tilde{u}_1) + \dots + f_{u_n}(\tilde{u}_1, \dots, \tilde{u}_n)(u_n - \tilde{u}_n).$$

If we let $\tilde{u}_1 = y_x$, $u_2 = y_{xx}$, $u_3 = y_{xxx}$, $u_4 = y_{xxxx}$ and use the above expansion,

we have

$$\begin{aligned} \frac{y_{xxxx}}{(1+y_x^2)^2} &= \frac{1}{(1+\tilde{y}_x^2)^2} \cdot y_{xxxx} - \frac{4\tilde{y}_x\tilde{y}_{xxxx}}{(1+\tilde{y}_x^2)^3} \cdot y_x + \frac{4\tilde{y}_x^2\tilde{y}_{xxxx}}{(1+\tilde{y}_x^2)^3} \\ \frac{y_x y_{xx} y_{xxx}}{(1+y_x^2)^3} &= -\frac{\tilde{y}_{xx}\tilde{y}_{xxx}(5\tilde{y}_x^2-1)}{(1+\tilde{y}_x^2)^4} \cdot y_x + \frac{\tilde{y}_x\tilde{y}_{xxx}}{(1+\tilde{y}_x^2)^3} \cdot y_{xx} \\ &\quad + \frac{\tilde{y}_x\tilde{y}_{xx}}{(1+\tilde{y}_x^2)^3} \cdot y_{xxx} + \frac{2\tilde{y}_x\tilde{y}_{xx}\tilde{y}_{xxx}(2\tilde{y}_x^2-1)}{(1+\tilde{y}_x^2)^4} \\ \frac{y_{xx}^3(5y_x^2-1)}{(1+y_x^2)^4} &= \frac{3\tilde{y}_{xx}^2(5\tilde{y}_x^2-1)}{(1+\tilde{y}_x^2)^4} \cdot y_{xx} + \frac{6\tilde{y}_x\tilde{y}_{xx}^3(3-5\tilde{y}_x^2)}{(1+\tilde{y}_x^2)^5} \cdot y_x \\ &\quad + \left[-\frac{2\tilde{y}_{xx}^3(5\tilde{y}_x^2-1)}{(1+\tilde{y}_x^2)^4} - \frac{6\tilde{y}_x\tilde{y}_{xx}^3(3-5\tilde{y}_x^2)}{(1+\tilde{y}_x^2)^5} \right] \end{aligned}$$

Thus, Equation (2.2) becomes

$$\begin{aligned}
\frac{\partial y_i}{\partial t} = & -B \left\{ \left[\frac{1}{(1 + \tilde{y}_x^2)^2} \right] y_{xxxx} + \left[-\frac{10\tilde{y}_x\tilde{y}_{xx}}{(1 + \tilde{y}_x^2)^3} \right] y_{xxx} \right. \\
& + \left[-\frac{10\tilde{y}_x\tilde{y}_{xxx}}{(1 + \tilde{y}_x^2)^3} + \frac{9\tilde{y}_{xx}^2(5\tilde{y}_x^2 - 1)}{(1 + \tilde{y}_x^2)^4} \right] y_{xx} \\
& + \left[-\frac{4\tilde{y}_x\tilde{y}_{xxxx}}{(1 + \tilde{y}_x^2)^3} + \frac{10\tilde{y}_{xx}\tilde{y}_{xxx}(5\tilde{y}_x^2 - 1)}{(1 + \tilde{y}_x^2)^4} + \frac{18\tilde{y}_x\tilde{y}_{xx}^3(3 - 5\tilde{y}_x^2)}{(1 + \tilde{y}_x^2)^5} \right] y_x \\
& \left. + \left[\frac{4\tilde{y}_x^2\tilde{y}_{xxxx}}{(1 + \tilde{y}_x^2)^3} - \frac{20\tilde{y}_x\tilde{y}_{xx}\tilde{y}_{xxx}(2\tilde{y}_x^2 - 1)}{(1 + \tilde{y}_x^2)^4} - \frac{6\tilde{y}_{xx}^3(5\tilde{y}_x^2 - 1)}{(1 + \tilde{y}_x^2)^4} - \frac{18\tilde{y}_x^2\tilde{y}_{xx}^3(3 - 5\tilde{y}_x^2)}{(1 + \tilde{y}_x^2)^5} \right] \right\}. \tag{4.10}
\end{aligned}$$

Using symmetry finite difference formulae with spatial derivative terms in Equation (4.10),

we have

$$\begin{aligned}
\frac{\partial y_i}{\partial t} = & -B \left\{ \left[\frac{1}{(1 + \tilde{y}_x^2)^2} \right] \left(\frac{y_{i+2} - 4y_{i+1} + 6y_i - 4y_{i-1} + y_{i-2}}{h^4} \right) \right. \\
& + \left[-\frac{10\tilde{y}_x\tilde{y}_{xx}}{(1 + \tilde{y}_x^2)^3} \right] \left(\frac{y_{i+2} - 2y_{i+1} + 2y_{i-1} - y_{i-2}}{2h^3} \right) \\
& + \left[-\frac{10\tilde{y}_x\tilde{y}_{xxx}}{(1 + \tilde{y}_x^2)^3} + \frac{9\tilde{y}_{xx}^2(5\tilde{y}_x^2 - 1)}{(1 + \tilde{y}_x^2)^4} \right] \left(\frac{y_{i+1} - 2y_i + y_{i-1}}{h^2} \right) \\
& + \left[-\frac{4\tilde{y}_x\tilde{y}_{xxxx}}{(1 + \tilde{y}_x^2)^3} + \frac{10\tilde{y}_{xx}\tilde{y}_{xxx}(5\tilde{y}_x^2 - 1)}{(1 + \tilde{y}_x^2)^4} + \frac{18\tilde{y}_x\tilde{y}_{xx}^3(3 - 5\tilde{y}_x^2)}{(1 + \tilde{y}_x^2)^5} \right] \left(\frac{y_{i+1} - y_{i-1}}{2h} \right) \\
& \left. + \left[\frac{4\tilde{y}_x^2\tilde{y}_{xxxx}}{(1 + \tilde{y}_x^2)^3} - \frac{20\tilde{y}_x\tilde{y}_{xx}\tilde{y}_{xxx}(2\tilde{y}_x^2 - 1)}{(1 + \tilde{y}_x^2)^4} - \frac{6\tilde{y}_{xx}^3(5\tilde{y}_x^2 - 1)}{(1 + \tilde{y}_x^2)^4} - \frac{18\tilde{y}_x^2\tilde{y}_{xx}^3(3 - 5\tilde{y}_x^2)}{(1 + \tilde{y}_x^2)^5} \right] \right\} \tag{4.11}
\end{aligned}$$

where $i = 1, 2, \dots, n$. Taking the Laplace transform of Equation (4.11) with respect to time

and rearranging terms yields

$$\begin{aligned}
\hat{y}_i - y(x, 0) = & -B \left\{ \left[\frac{1}{h^4(1 + \tilde{y}_x^2)^2} - \frac{5\tilde{y}_x\tilde{y}_{xx}}{h^3(1 + \tilde{y}_x^2)^3} \right] \hat{y}_{i+2} \right. \\
& + \left[-\frac{4}{h^4(1 + \tilde{y}_x^2)^2} + \frac{10\tilde{y}_x\tilde{y}_{xx}}{h^3(1 + \tilde{y}_x^2)^3} - \frac{10\tilde{y}_x\tilde{y}_{xxx}}{h^2(1 + \tilde{y}_x^2)^3} + \frac{9\tilde{y}_{xx}^2(5\tilde{y}_x^2 - 1)}{h^2(1 + \tilde{y}_x^2)^4} \right. \\
& \left. \left. - \frac{2\tilde{y}_x\tilde{y}_{xxxx}}{h(1 + \tilde{y}_x^2)^3} + \frac{5\tilde{y}_{xx}\tilde{y}_{xxx}(5\tilde{y}_x^2 - 1)}{h(1 + \tilde{y}_x^2)^4} + \frac{9\tilde{y}_x\tilde{y}_{xx}^3(3 - 5\tilde{y}_x^2)}{h(1 + \tilde{y}_x^2)^5} \right] \hat{y}_{i+1} \right. \\
& + \left[\frac{6}{h^4(1 + \tilde{y}_x^2)^2} + \frac{20\tilde{y}_x\tilde{y}_{xxx}}{h^2(1 + \tilde{y}_x^2)^3} - \frac{18\tilde{y}_{xx}^2(5\tilde{y}_x^2 - 1)}{h^2(1 + \tilde{y}_x^2)^4} \right] \hat{y}_i \\
& + \left[-\frac{4}{h^4(1 + \tilde{y}_x^2)^2} - \frac{10\tilde{y}_x\tilde{y}_{xx}}{h^3(1 + \tilde{y}_x^2)^3} - \frac{10\tilde{y}_x\tilde{y}_{xxx}}{h^2(1 + \tilde{y}_x^2)^3} + \frac{9\tilde{y}_{xx}^2(5\tilde{y}_x^2 - 1)}{h^2(1 + \tilde{y}_x^2)^4} \right. \\
& \left. + \frac{2\tilde{y}_x\tilde{y}_{xxxx}}{h(1 + \tilde{y}_x^2)^3} - \frac{5\tilde{y}_{xx}\tilde{y}_{xxx}(5\tilde{y}_x^2 - 1)}{h(1 + \tilde{y}_x^2)^4} - \frac{9\tilde{y}_x\tilde{y}_{xx}^3(3 - 5\tilde{y}_x^2)}{h(1 + \tilde{y}_x^2)^5} \right] \hat{y}_{i-1} \\
& + \left[\frac{1}{h^4(1 + \tilde{y}_x^2)^2} + \frac{5\tilde{y}_x\tilde{y}_{xx}}{h^3(1 + \tilde{y}_x^2)^3} \right] \hat{y}_{i-2} \\
& + \left[\frac{4\tilde{y}_x\tilde{y}_{xxxx}}{(1 + \tilde{y}_x^2)^3} - \frac{20\tilde{y}_x\tilde{y}_{xx}\tilde{y}_{xxx}(2\tilde{y}_x^2 - 1)}{(1 + \tilde{y}_x^2)^4} - \frac{6\tilde{y}_{xx}^3(5\tilde{y}_x^2 - 1)}{(1 + \tilde{y}_x^2)^4} \right. \\
& \left. \left. - \frac{18\tilde{y}_x\tilde{y}_{xx}^3(3 - 5\tilde{y}_x^2)}{(1 + \tilde{y}_x^2)^5} \right] \left(\frac{1}{s} \right) \right\}. \tag{4.12}
\end{aligned}$$

Doing the same way with the boundary conditions, finally we will obtain

$$\begin{aligned}
\hat{y}_0 &= \hat{y}_2 - \frac{2mh}{s}, \\
\hat{y}_{n+1} &= \hat{y}_{n-1}, \\
\hat{y}_{-1} &= \frac{24h\tilde{y}_x\tilde{y}_{xx}}{1 + \tilde{y}_x^2} \cdot \hat{y}_1 - \frac{24h\tilde{y}_x\tilde{y}_{xx}}{1 + \tilde{y}_x^2} \cdot \hat{y}_2 + \hat{y}_3 + \left(\frac{1}{s} \right) \left[-4mh + \frac{2h^3}{1 + \tilde{y}_x^2} \right. \\
& \left. \left(\frac{12m\tilde{y}_x\tilde{y}_{xx}}{h} + 2m\tilde{y}_x\tilde{y}_{xxx} - 3m\tilde{y}_{xx}^2 + 6\tilde{y}_x\tilde{y}_{xx}^2 - 2\tilde{y}_x\tilde{y}_{xxx} \right) \right], \\
\hat{y}_{n+2} &= \hat{y}_{n-2} + \frac{24h\tilde{y}_x\tilde{y}_{xx}}{1 + \tilde{y}_x^2} \cdot \hat{y}_{n-1} - \frac{24h\tilde{y}_x\tilde{y}_{xx}}{1 + \tilde{y}_x^2} \cdot \hat{y}_n - \left(\frac{1}{s} \right) \left[\frac{2h^3}{1 + \tilde{y}_x^2} \left(6\tilde{y}_x\tilde{y}_{xx}^2 - 2\tilde{y}_x\tilde{y}_{xxx} \right) \right]. \tag{4.13}
\end{aligned}$$

We can now solve system (4.8) or (4.12) together with Equation (4.9) or (4.13) as

described in Section 3.3. However, instead of solving linear system (4.8) or (4.12) together with (4.9) or (4.13) by standard Gaussian elimination, we will solve it by Thomas' algorithm for pentadiagonal matrix which will save time greatly.

From Figures 4.11 and 4.12, one can see that LTFDM based on both direct linearization scheme and Taylor series expansion linearization scheme, called LTFDM-D and LTFDM-T respectively, give groove profiles which are in very good agreement with T&B's. When the slope at the groove root $m = 0.7$, LTFDM-T produces better result than LTFDM-D does (see Figure 4.13). When increasing the slope at the groove root above 0.7, the shape of the groove is still correct but it is lower than T&B's (see Figures 4.15 - 4.19). For LTFDM-D, we can increase the number of nodes if we want to increase the accuracy. Here, we choose approximately 30-60 nodal points for $m < 1$ and 400-1000 nodal points for $m \geq 1$. On the other hand, we can choose only 20-35 nodal points for LTFDM-T for all the value of m presented. It is rather strange that the larger the groove slope is the less nodal points can be used in LTFDM-T. For example, at the groove root $m = 0.1$, the maximum of nodal points is $N = 35$ and for $m = 3$, $N = 20$.

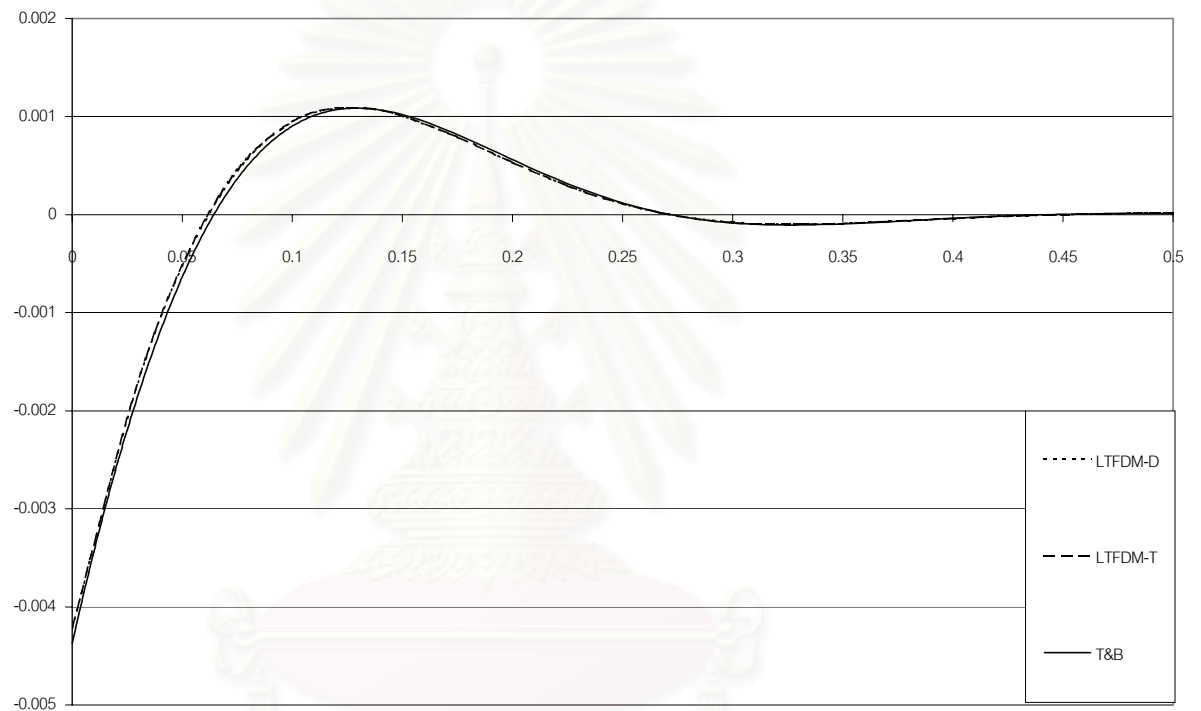


Figure 4.11: Comparison of groove profiles produced from LTFDM-D (dotted line), LTFDM-T (dashed line), and T&B's solution (solid line) for $m = 0.1$.

จุฬาลงกรณ์มหาวิทยาลัย

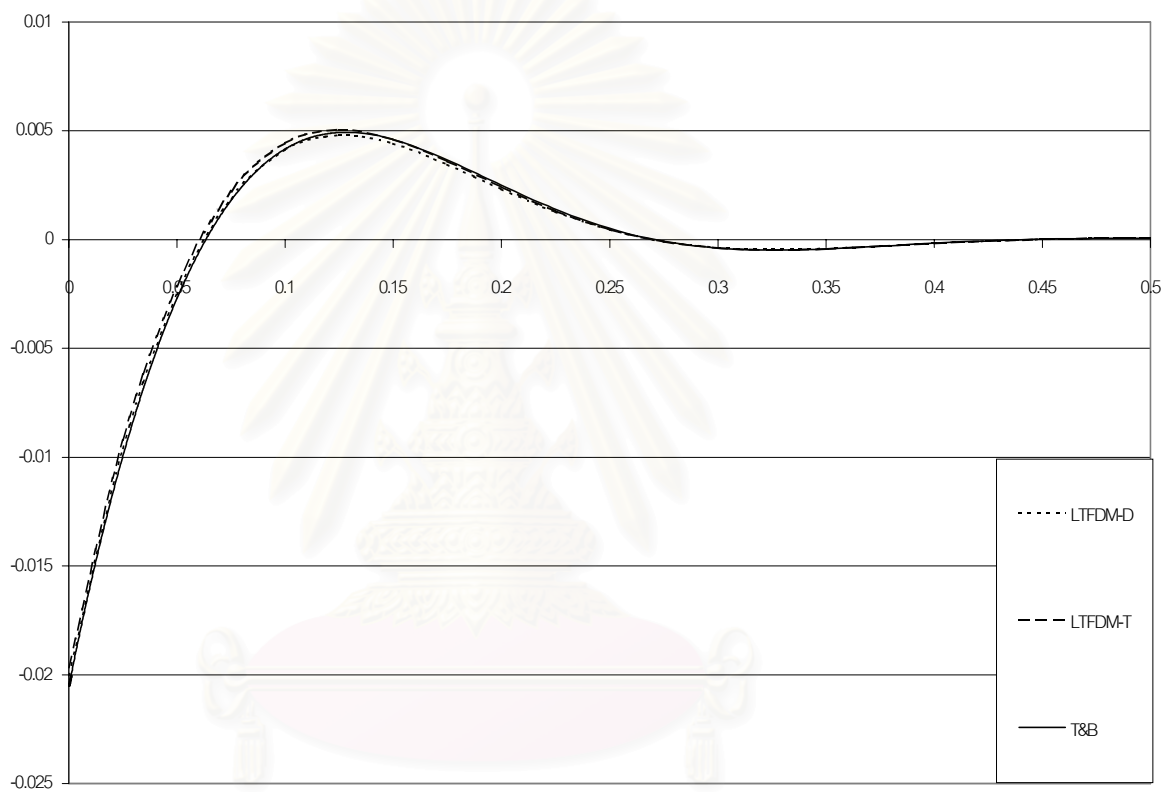


Figure 4.12: Comparison of groove profiles produced from LTFDM-D (dotted line), LTFDM-T (dashed line), and T&B's solution (solid line) for $m = 0.5$.

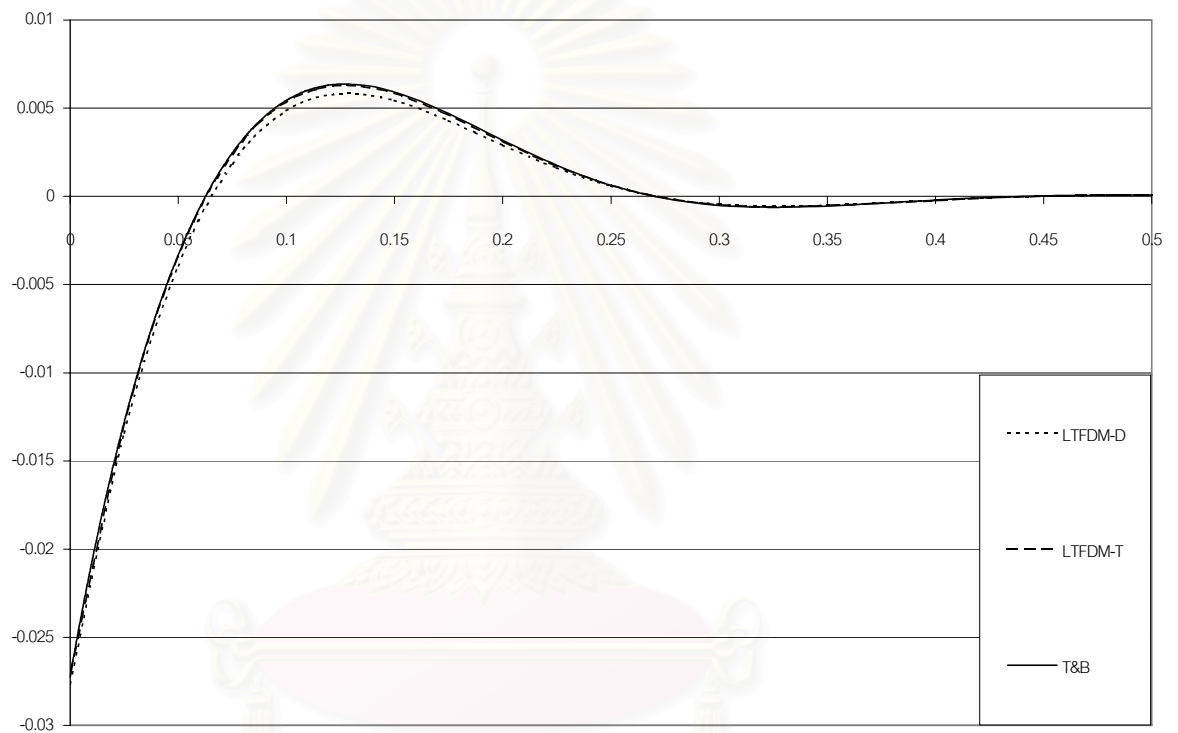


Figure 4.13: Comparison of groove profiles produced from LTFDM-D (dotted line), LTFDM-T (dashed line), and T&B's solution (solid line) for $m = 0.7$.

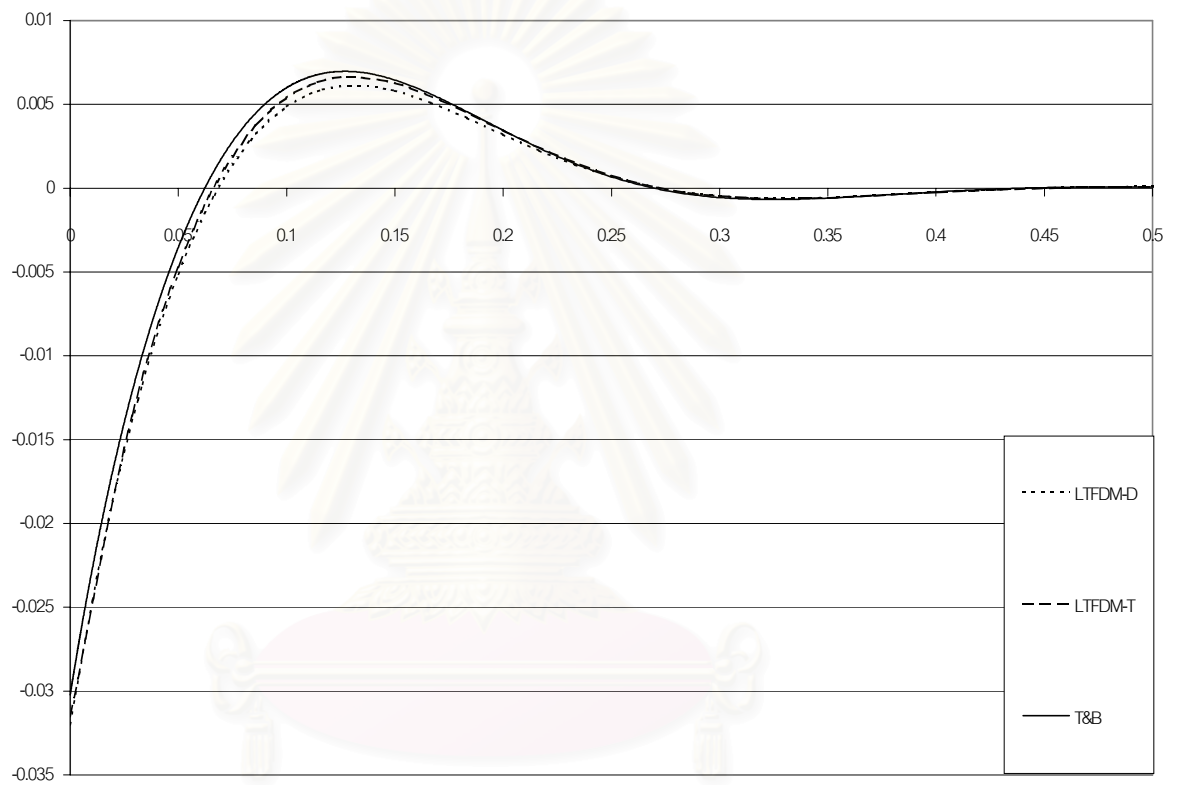


Figure 4.14: Comparison of groove profiles produced from LTFDM-D (dotted line), LTFDM-T (dashed line), and T&B's solution (solid line) for $m = 0.8$.

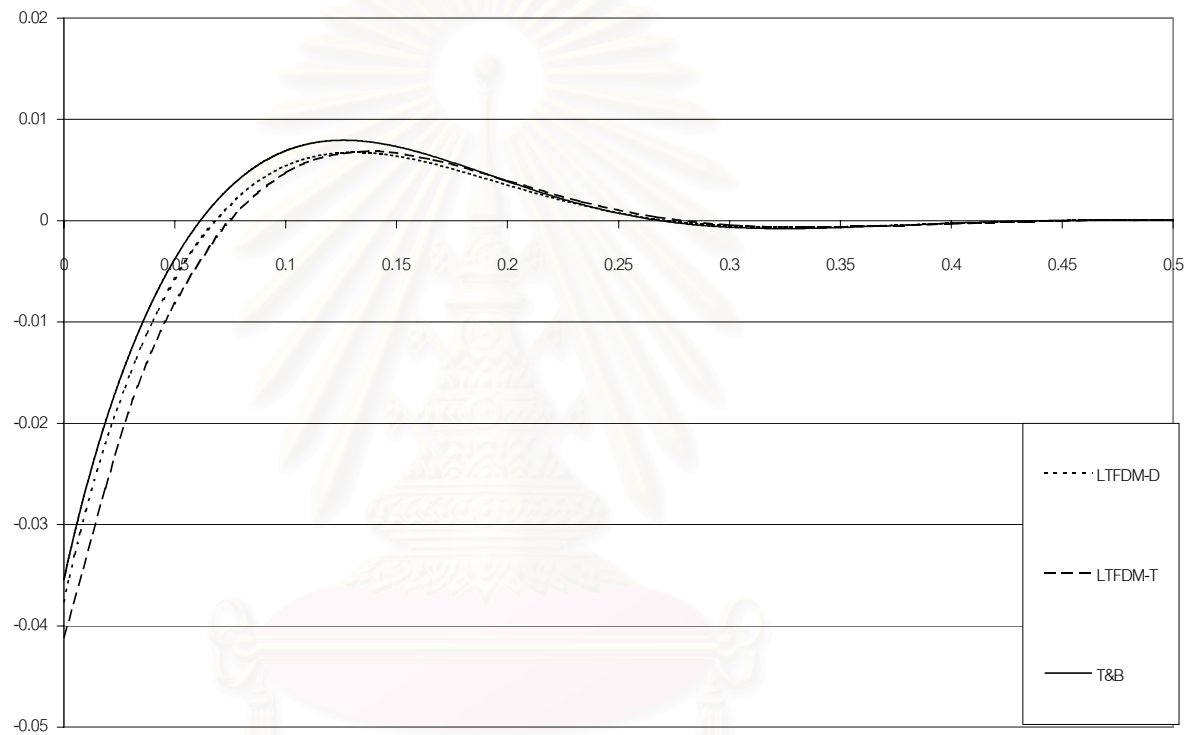


Figure 4.15: Comparison of groove profiles produced from LTFDM-D (dotted line), LTFDM-T (dashed line), and T&B's solution (solid line) for $m = 1.0$.

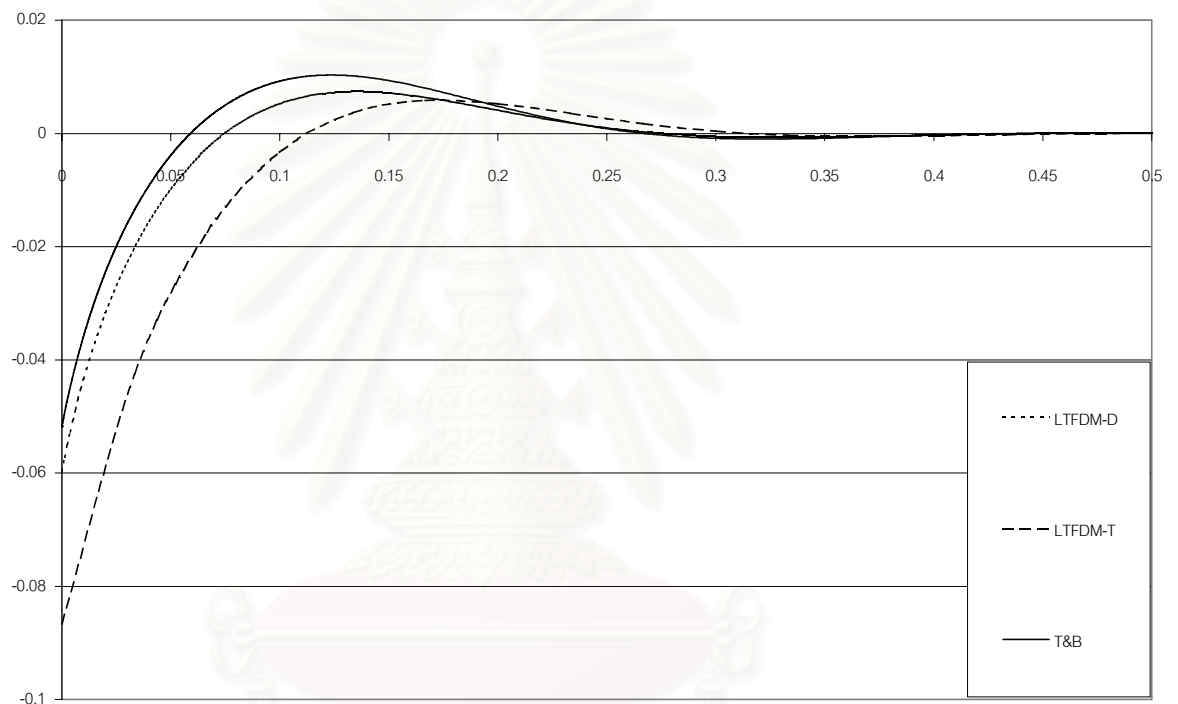


Figure 4.16: Comparison of groove profiles produced from LTFDM-D (dotted line), LTFDM-T (dashed line), and T&B's solution (solid line) for $m = 2.0$.

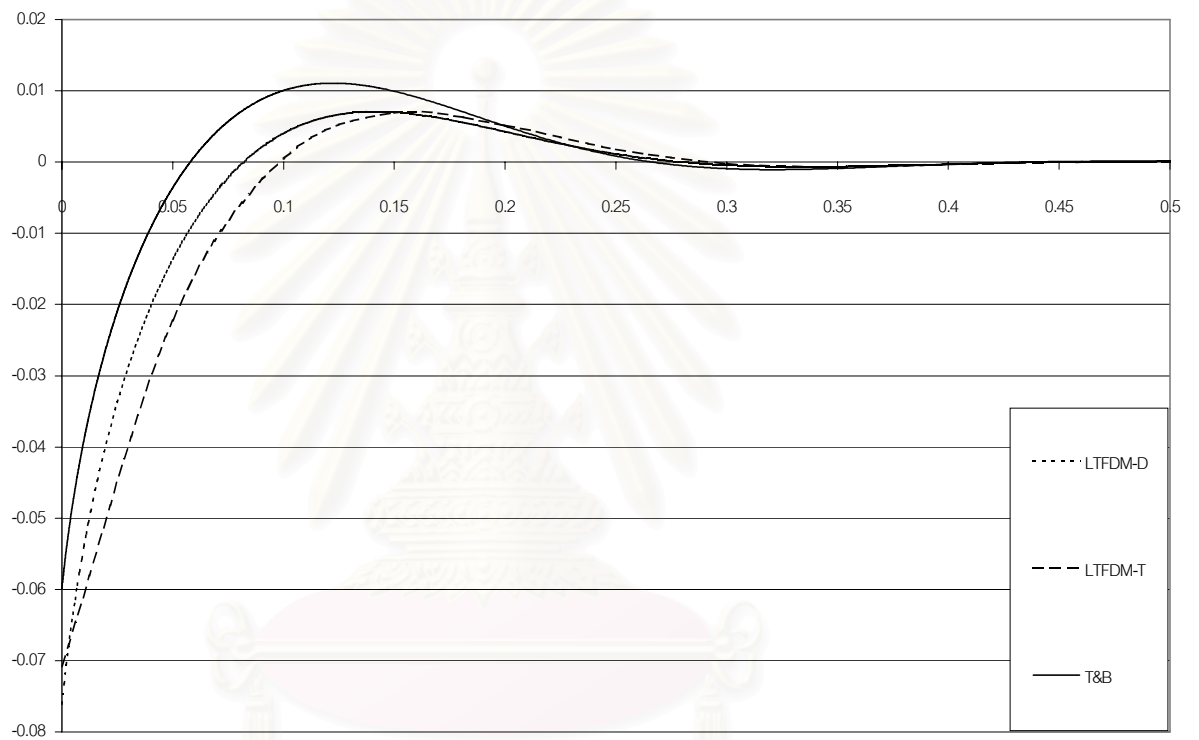


Figure 4.17: Comparison of groove profiles produced from LTFDM-D (dotted line), LTFDM-T (dashed line), and T&B's solution (solid line) for $m = 3.0$.

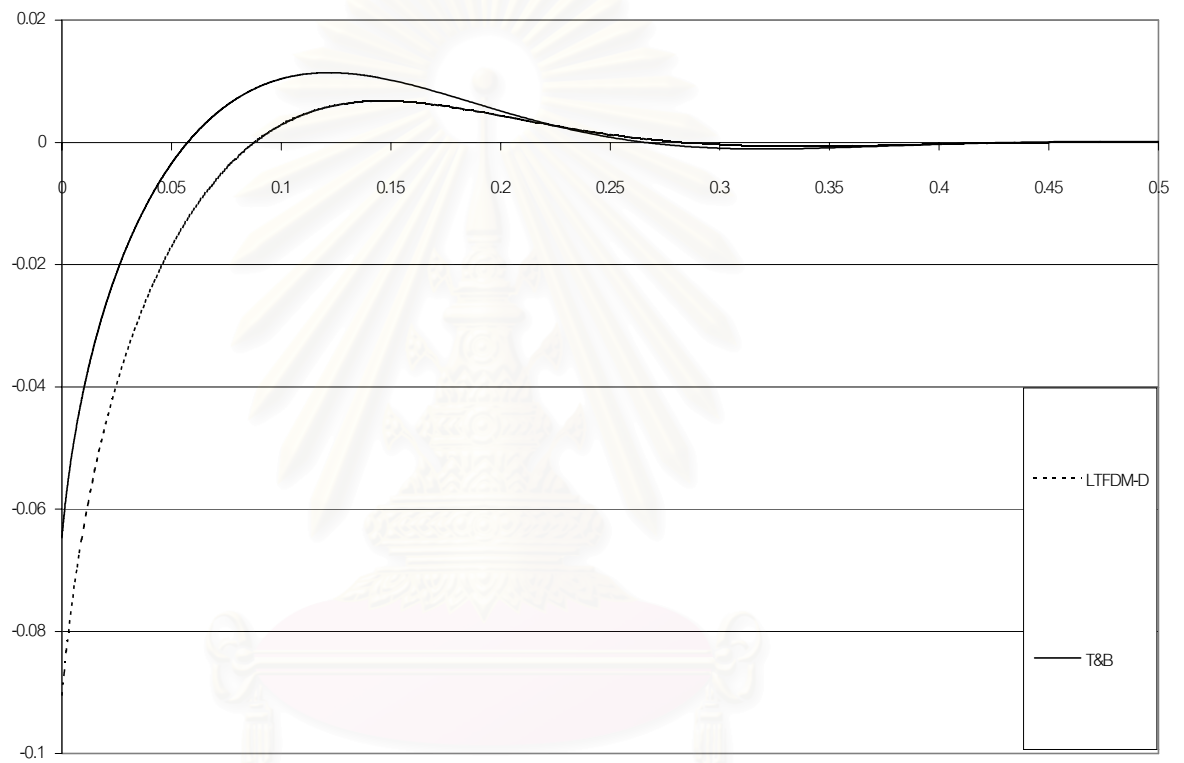


Figure 4.18: Comparison of groove profiles produced from LTFDM-D (dotted line), LTFDM-T (dashed line), and T&B's solution (solid line) for $m = 4.0$.

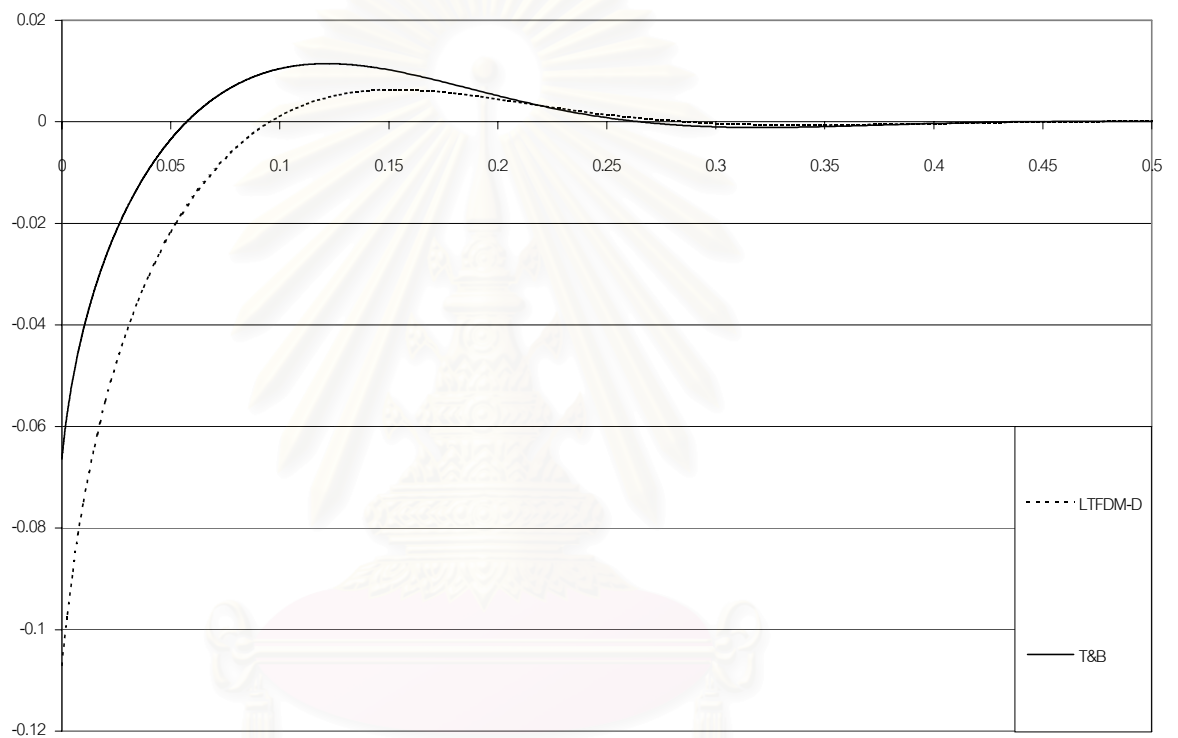


Figure 4.19: Comparison of groove profiles produced from LTFDM-D (dotted line), LTFDM-T (dashed line), and T&B's solution (solid line) for $m = 4.5$.

4.4 Comparison

Figures 4.20 and 4.21 show that all numerical methods presented herein give similar results that are in excellent agreement with T&B's solution when $m = 0.1$ and $m = 0.5$. For better comparison, we calculate relative error of solution produced by each method at 10 points which are equally spreaded over $[0, 0.45]$. Then we take an average of these relative errors, which is denoted ARE. The relative error is computed based on L_∞ -norm. From Table 4.1, when $m = 0.5$, every method gives the solution with ARE less than 10%. But, when $m = 0.7$, LTFDM-T produces the best accurate solution compared with T&B's solution with ARE = 8.51% while the others have ARE more than 10%. Additionally, LTFDM-D and LTFDM-T give better results than the others for $m = 0.8$. Moreover, for $m = 1$, LTFDM-D gives the solution which is closest to T&B's solution (see Figure 4.24). Furthermore, when the value of m is increased, the number of nodal points has to be increased accordingly for more accuracy, which can be done quickly and easily by LTFDM. On the other hand, for cubic splines and finite difference methods, we have to increase a great deal of time steps also.

m	CBS	Liu	FDM	LTFDM-D	LTFDM-T
0.5	5.97	7.06	5.32	8.05	9.98
0.7	17.99	16.62	18.61	11.36	8.51
0.8	33.51	32.15	28.09	17.52	17.71

Table 4.1 : The average relative errors.

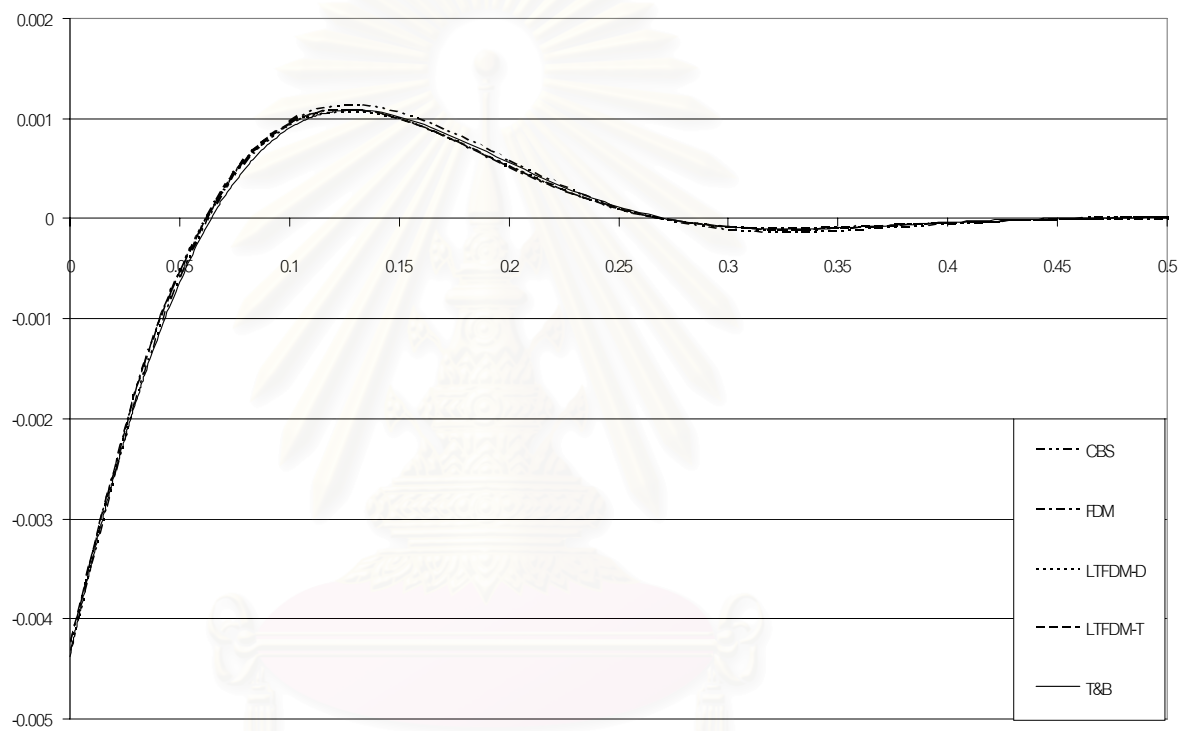


Figure 4.20: Comparison between each numerical method for solving non-linear Mullins equation when $m = 0.1$.

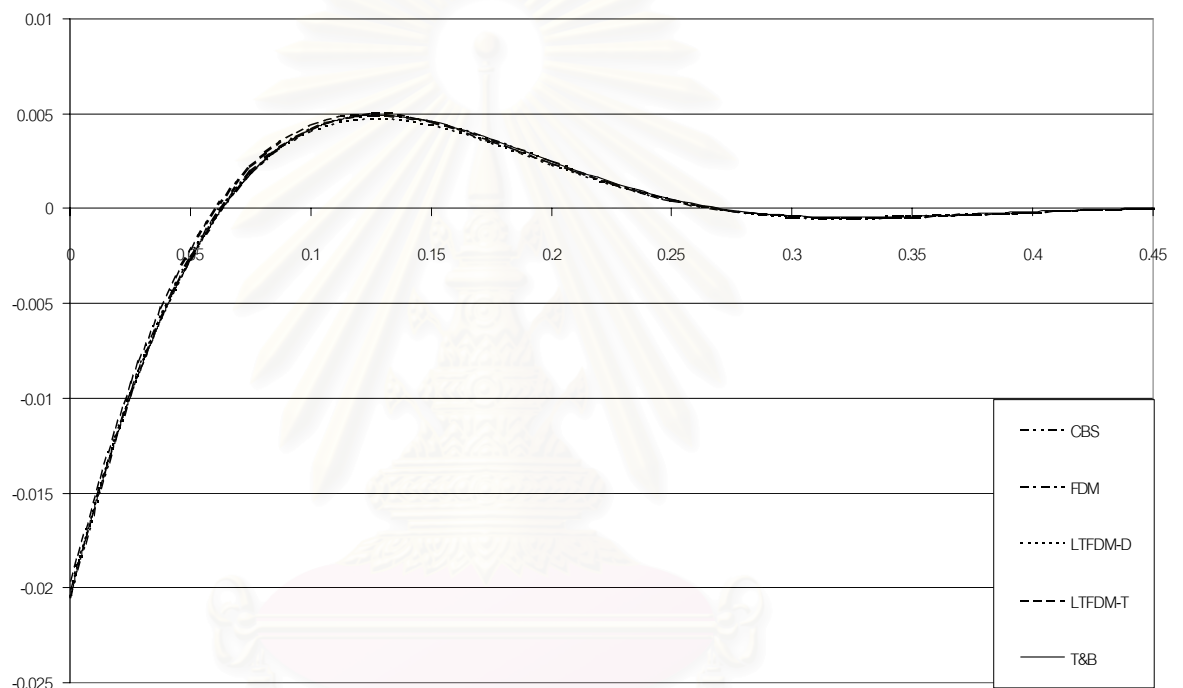


Figure 4.21: Comparison between each numerical method for solving non-linear Mullins equation when $m = 0.5$.

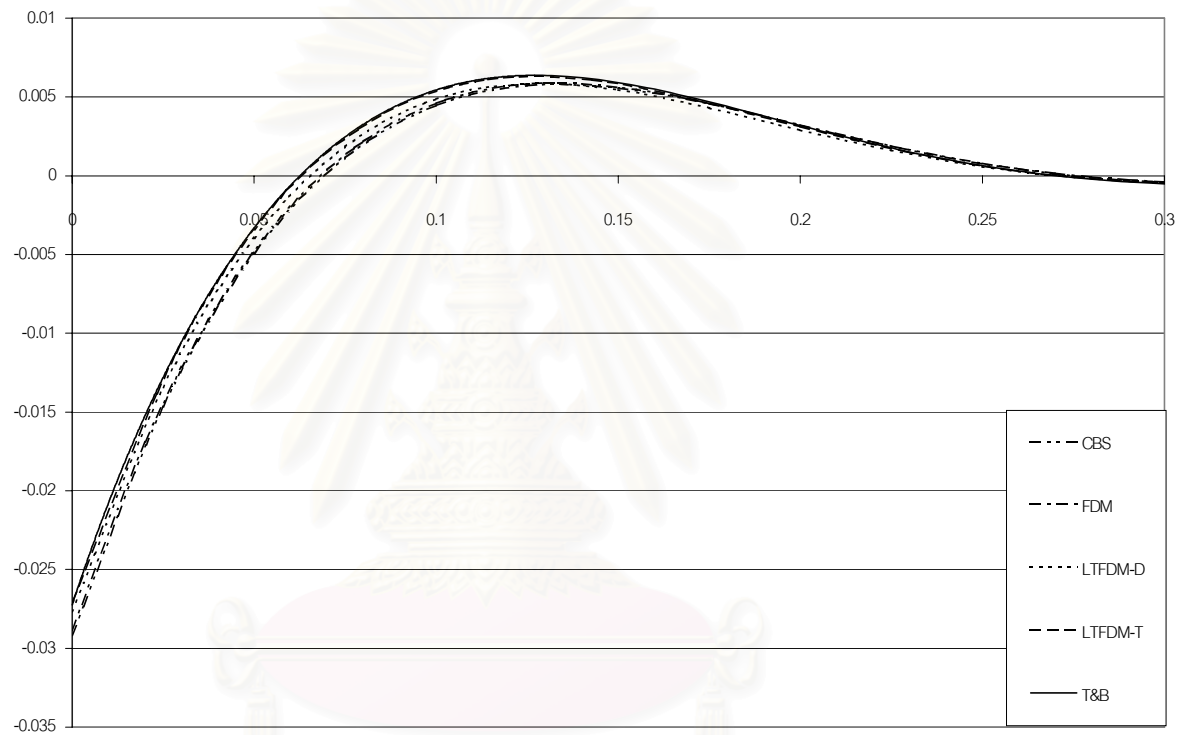


Figure 4.22: Comparison between each numerical method for solving non-linear Mullins equation when $m = 0.7$.

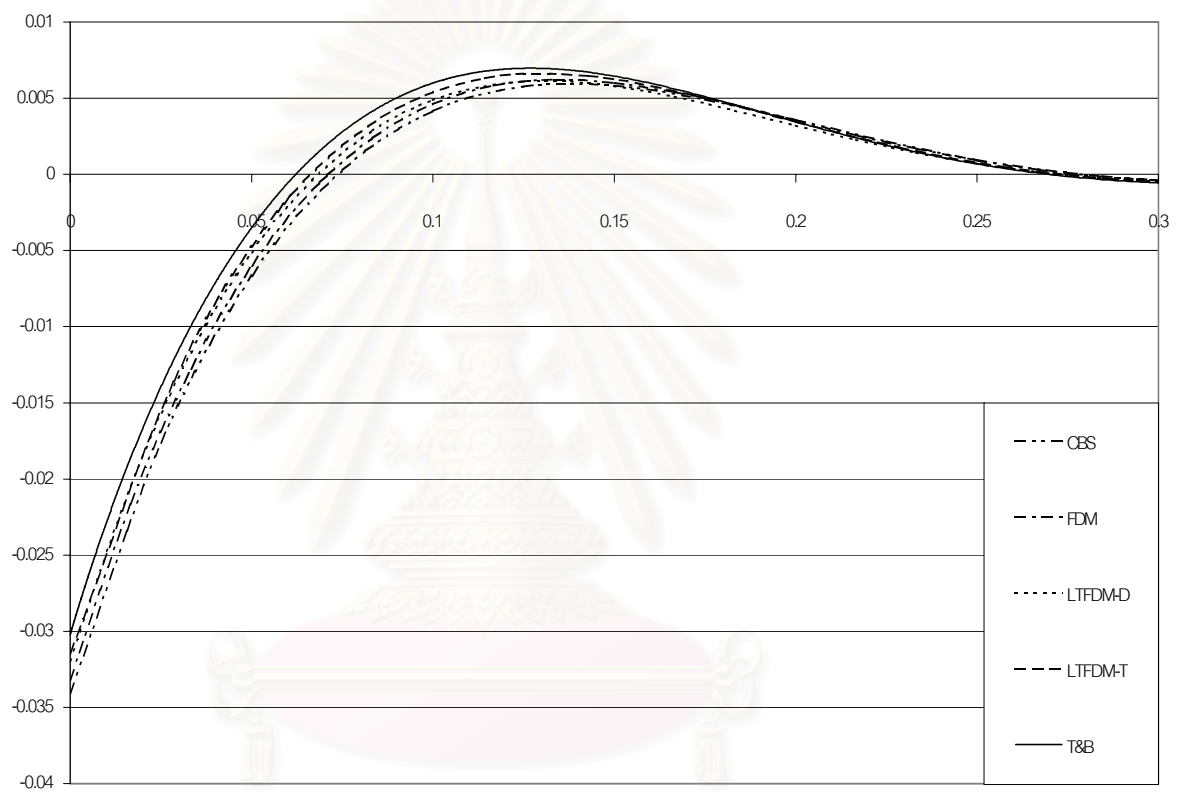


Figure 4.23: Comparison between each numerical method for solving non-linear Mullins equation when $m = 0.8$.

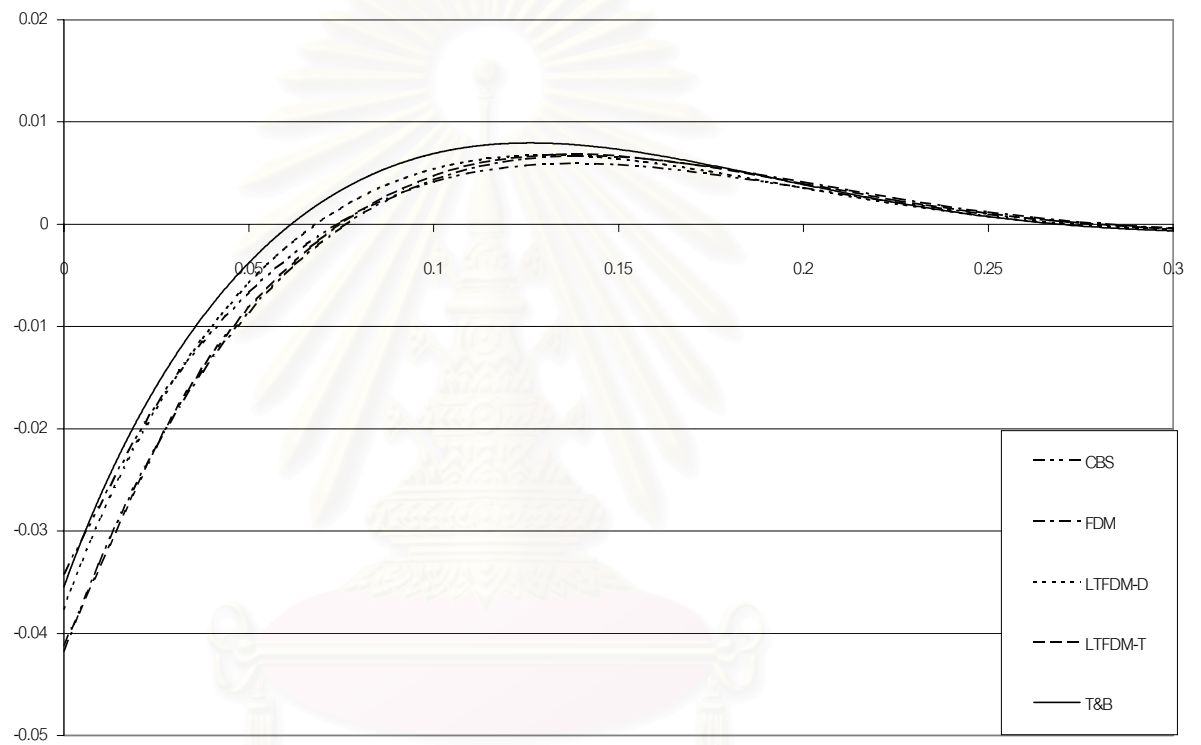


Figure 4.24: Comparison between each numerical method for solving non-linear Mullins equation when $m = 1.0$.

Chapter 5

Conclusion

In this thesis, three numerical approaches including cubic splines method, finite difference method (FDM), and Laplace transform finite difference method (LTFDM) are presented and applied to solve Mullins equation which is the fourth-order non-linear partial differential equation describing grain boundary grooving by surface diffusion. All methods are first tested with linearized Mullins equation before extended to non-linear case. Numerical results produced by these three methods exhibit very good accuracy compared with exact solution of linear Mullins equation. However, our main aim is to extend all the methods to solving non-linear Mullins equation.

Cubic splines method was previously used to solve Mullins equation by Liu [7]. Herein, we solve Mullins equation by cubic splines method through slightly changing Liu's derivation and compare our results with the solution obtained via Liu's derivation. We find that the result from our derivation is similar to that from Liu's derivation, and the accuracy is very good when the groove slope is not more than 0.5 compared to T&B's solution.

Also, FDM was previously used to solve Mullins equation by Lee [6]. Our work is to study this numerical technique for Mullins equation. We find that the result is in very good agreement with T&B's solution for the groove slope $m \leq 0.5$.

The highlight of this thesis is to solve Mullins equation by LTFDM through direct linearization and Taylor series expansion schemes. By the way of LTFDM, we have to use the numerical inversion of Laplace transform. Herein, the numerical inversion of Laplace transform called "Stehfest's algorithm" is utilized. The results obtained from LTFDM based on direct linearization scheme, called LTFDM-D, are presented for the groove slope ranging between 0 and 4.5. Additionally, LTFDM-D's solution agrees very well with T&B's solution when the groove slope is not more than 0.5. For LTFDM based on Taylor series expansion linearization scheme, denoted LTFDM-T, the numerical results obtained compare very well with T&B's solution when the groove slope is not more than 0.7 which is better than the other methods. Moreover, for the groove slope $m = 0.8$, LTFDM-D and LTFDM-T produce better accurate results than the other methods do. Unfortunately, LTFDM-T somehow fails when the value of m is beyond 3.

For the time used in calculation, LTFDM uses the time much less than cubic splines method and FDM because LTFDM does not have to calculate at each time step. Therefore, we can quickly obtain an accurate solution at any specific time by LTFDM. On the other hand, cubic splines method and FDM spend time for calculating at each time step. Moreover, if we want to increase the number of nodes for more accuracy, it can be done easily with LTFDM. For cubic splines and FDM, we have to increase the number of time step also so that the time for calculation is increased at the same time.

From all of the points mentioned above, LTFDM is a powerful numerical method for solving Mullins equation and LTFDM-T is better than LTFDM-D for small slope, $m < 1$, and LTFDM-D is better than LTFDM-T for larger slope, $1 \leq m \leq 4.5$. However, there are many methods for numerical inversion of Laplace transform. For the future works, LTFDM may be improved by using other numerical inversion of Laplace transform and extended to solving other non-linear partial differential equations.



สถาบันวิทยบริการ
จุฬาลงกรณ์มหาวิทยาลัย

References

- [1] Mullins, W. W. Theory of hermal grooving, *J. Appl. Phys.*, 1957, **28**, 333-339.
- [2] Robertson, W. M. Grain-boundary grooving by surface diffusion for finite surface slopes, *J. Appl. Phys.*, 1971, **42**, 463-467.
- [3] Zhang, W. and Schneibel, J. H. Numerical simulation of grain-boundary grooving by surface diffusion, *Computational Materials Science*, 1995, **3**, 347-358.
- [4] Cahn, J. W. and Taylor, J. E. Surface motion by surface diffusion, *Acta Metall. Mater.*, 1994, **42**, 1045-1063.
- [5] Tritscher, P. and Broadbridge, P. Grain boundary grooving by surface diffusion: an analytic nonlinear model for a symmetric groove, *Proc. R. Soc. Lond. A*, 1995, **450**, 569-587.
- [6] Lee, M. Z. C. A numerical model for dominant surface diffusion applied to periodic sputtering of surfaces, Honours Thesis, Dept. of Mathematics, University of Wollongong Australia, 1995.

- [7] Liu, S. Solving PDE with Cubic Splines, Dept. of Mathematics, University of Wollongong, Australia, 2000.
- [8] Stehfest, H. Algorithm 368: numerical inversion of Laplace transform, *Comm. ACM*, 1970, **13**, 47-49 and 624.
- [9] Chen, H. T. and Chen, C. K. Hybrid Laplace transform/finite difference method for transient heat conduction problems, *Int. J. Numer. Methods Eng.*, 1988, **26**, 1433-1447.
- [10] Chen, H. T. and Lin, J. Y. Application of the Laplace transform to nonlinear transient problems, *Appl. Math. Modelling*, 1991, **15**, 144-151.
- [11] Satravaha, P. Solving linear and nonlinear transient diffusion problems with Laplace transform dual reciprocity method, Ph.D. thesis, Dept. of Mathematics, University of Wollongong, Australia, 1996.
- [12] Zhu, S., Satravaha, P., and Lu, X. Solving linear diffusion equations with the dual reciprocity method in Laplace space, *Engineering Analysis with Boundary Elements*, 1994, **13**, 1-10.
- [13] Prenter, P. M. *Splines and variational methods*, Newyork, Wiley, 1975.
- [14] IMSL, *User's Manual*, MATH/Library, IMSL, Houston, 1991.

Appendix A

Exact solution for linear Mullins equation

For convenience, let $u(x, t) = y(x, t) + \frac{m}{2L}x^2 - mx$. The advantage of this change is to have homogeneous boundary conditions. Hence, the new system to be solved in terms of u is as follows:

$$u_t = -Bu_{xxxx} \quad (\text{A.1})$$

subject to

$$\text{IC. } u(x, 0) = \frac{m}{2L}x^2 - mx$$

$$\text{BC. } u_x(0, t) = 0,$$

$$u_{xxx}(0, t) = 0, \quad (\text{A.2})$$

$$u_x(L, t) = 0,$$

$$u_{xxx}(L, t) = 0.$$

Using separation of variables, let $u(x, t) = X(x)T(t)$ and substitute it in Equation (A.1).

So, we have

$$-\frac{1}{B} \frac{T'(t)}{T(t)} = \frac{X^{(4)}(x)}{X(x)} = k. \quad (\text{A.3})$$

Case 1. $k > 0$ (let $k = \lambda^4$, $\lambda > 0$)

From Equation (A.3), we have two ODE's, i.e.,

$$T'(t) + kBT(t) = 0,$$

and

$$X^{(4)}(x) - \lambda^4 X(x) = 0,$$

which have corresponding general solutions as

$$T(t) = d_1 e^{-kBt},$$

and

$$X(x) = c_1 e^{\lambda x} + c_2 e^{-\lambda x} + c_3 \cos \lambda x + c_4 \sin \lambda x.$$

From boundary conditions in Equation (A.2), we have

$$X'(0) = 0 \quad : \quad \lambda c_1 - \lambda c_2 + \lambda c_4 = 0$$

$$X'(L) = 0 \quad : \quad \lambda c_1 e^{\lambda L} - \lambda c_2 e^{-\lambda L} - \lambda c_3 \sin \lambda L + \lambda c_4 \cos \lambda L = 0$$

$$X'''(0) = 0 \quad : \quad \lambda^3 c_1 - \lambda^3 c_2 - \lambda^3 c_4 = 0$$

$$X'''(L) = 0 \quad : \quad \lambda^3 c_1 e^{\lambda L} - \lambda^3 c_2 e^{-\lambda L} + \lambda^3 c_3 \sin \lambda L - \lambda^3 c_4 \cos \lambda L = 0.$$

Solving for c_1 , c_2 , c_3 , and c_4 , we have $c_1 = c_2 = c_4 = 0$ and $c_3 \sin \lambda L = 0$. Since $c_3 \neq 0$, otherwise it gives trivial solution; $\sin \lambda L = 0$. Thus, $\lambda_n = \frac{n\pi}{L}$, $n = 1, 2, 3, \dots$ so that

$X_n(x) = c_n \cos \frac{n\pi x}{L}$ and $T_n(t) = d_n e^{-n^4 \pi^4 Bt/L^4}$. Hence,

$$\begin{aligned} u_n(x, t) &= X_n(x)T_n(t) \\ &= C_n e^{-n^4 \pi^4 Bt/L^4} \cos \frac{n\pi x}{L}, n = 1, 2, 3, \dots \end{aligned}$$

where $C_n = c_n d_n$.

Case 2. $k = 0$

From Equation (A.3), we have two ODE's, solutions of which are $T(t) = d_1$, and $X(x) = c_1 + c_2 x + c_3 x^2 + c_4 x^3$.

From boundary conditions in Equation (A.2), we have in this case

$$\begin{aligned} X'(0) = 0 & : c_2 = 0 \\ X'(L) = 0 & : c_2 + 2c_3 L + 3c_4 L^2 = 0 \\ X'''(0) = 0 & : 6c_4 = 0 \\ X'''(L) = 0 & : 6c_4 = 0. \end{aligned}$$

Solving this linear system of equations, we have $c_2 = c_3 = c_4 = 0$ and c_1 is an arbitrary constant. As a result, $X(x) = c_1$ and $T(t) = d_1$. Accordingly, $u(x, t) = c_1 d_1$. However, let us write it in another form as

$$u(x, t) = \frac{C_0}{2}.$$

Case 3. $k < 0$ (let $k = -\lambda^4$, $\lambda > 0$)

From Equation (A.3), we have two ODE's, solutions of which are $T(t) = d_1 e^{-k Bt}$, and $X(x) = e^{\frac{\sqrt{2}}{2} \lambda x} (c_1 \cos \frac{\sqrt{2}}{2} \lambda x + c_2 \sin \frac{\sqrt{2}}{2} \lambda x) + e^{-\frac{\sqrt{2}}{2} \lambda x} (c_3 \cos \frac{\sqrt{2}}{2} \lambda x + c_4 \sin \frac{\sqrt{2}}{2} \lambda x)$.

From boundary conditions in Equation (A.2), we have

$$\begin{aligned}
X'(0) = 0 & : c_1 + c_2 - c_3 + c_4 = 0 \\
X'(L) = 0 & : e^{\frac{\sqrt{2}}{2}\lambda L} [c_1(\cos \frac{\sqrt{2}}{2}\lambda L - \sin \frac{\sqrt{2}}{2}\lambda L) + c_2(\cos \frac{\sqrt{2}}{2}\lambda L + \sin \frac{\sqrt{2}}{2}\lambda L)] \\
& + e^{-\frac{\sqrt{2}}{2}\lambda L} [c_3(-\cos \frac{\sqrt{2}}{2}\lambda L - \sin \frac{\sqrt{2}}{2}\lambda L) + c_4(\cos \frac{\sqrt{2}}{2}\lambda L - \sin \frac{\sqrt{2}}{2}\lambda L)] = 0 \\
X'''(0) = 0 & : -c_1 + c_2 + c_3 + c_4 = 0 \\
X'''(L) = 0 & : e^{\frac{\sqrt{2}}{2}\lambda L} [c_1(-\cos \frac{\sqrt{2}}{2}\lambda L - \sin \frac{\sqrt{2}}{2}\lambda L) + c_2(\cos \frac{\sqrt{2}}{2}\lambda L - \sin \frac{\sqrt{2}}{2}\lambda L)] \\
& + e^{-\frac{\sqrt{2}}{2}\lambda L} [c_3(\cos \frac{\sqrt{2}}{2}\lambda L - \sin \frac{\sqrt{2}}{2}\lambda L) + c_4(\cos \frac{\sqrt{2}}{2}\lambda L + \sin \frac{\sqrt{2}}{2}\lambda L)] = 0.
\end{aligned}$$

Solving this linear system of equations, we have $c_1 = c_2 = c_3 = c_4 = 0$. Hence,

$$u(x, t) = 0.$$

From 3 cases, the solution of Equation (A.1) satisfying boundary conditions in Equation (A.2) is

$$u(x, t) = \frac{C_0}{2} + \sum_{n=1}^{\infty} C_n e^{-n^4 \pi^4 B t / L^4} \cos \frac{n \pi x}{L}.$$

Applying initial condition yields

$$\frac{m}{2L} x^2 - mx = \frac{C_0}{2} + \sum_{n=1}^{\infty} C_n \cos \frac{n \pi x}{L},$$

which is the half-range expansion of $\frac{m}{2L} x^2 - mx$ in the interval $[0, L]$. Thus, from Fourier cosine series, we obtain $C_0 = -\frac{2mL}{3}$ and $C_n = \frac{2mL}{(n\pi)^2}$, $n = 1, 2, 3, \dots$. Therefore,

$$u(x, t) = -\frac{mL}{3} + \sum_{n=1}^{\infty} \frac{2mL}{(n\pi)^2} e^{-n^4 \pi^4 B t / L^4} \cos \frac{n \pi x}{L}$$

so that the actual analytical solution is

$$y(x, t) = -\frac{mx^2}{2L} + mx - \frac{mL}{3} + \sum_{n=1}^{\infty} \frac{2mL}{(n\pi)^2} e^{-n^4 \pi^4 B t / L^4} \cos \frac{n \pi x}{L}.$$

Mullins [1], on the other hand, solved the exact solution from

$$\frac{\partial y}{\partial t} + By_{xxxx} = 0 \quad (\text{A.4})$$

subject to

$$\begin{aligned} \text{IC. } & y(x, 0) = 0 \\ \text{BC. } & y_x(0, t) = m, \\ & y_{xxx}(0, t) = 0. \end{aligned} \quad (\text{A.5})$$

Using the Laplace transform technique together with initial condition from Equation (A.5), we operate on Equation (A.4) in the usual way to obtain

$$By_{xxxx} + sy = 0, \quad (\text{A.6})$$

where s is the Laplace parameter. Boundary conditions from Equation (A.5) are transformed into

$$\hat{y}_x(0, s) = m/s, \quad (\text{A.7})$$

and

$$\hat{y}_{xxx}(0, s) = 0. \quad (\text{A.8})$$

The solution of Equation (A.6) that behaves properly at infinity and obeys conditions (A.7) and (A.8), is found by standard methods to be

$$\hat{y} = \frac{mB^{1/4}}{s^{5/4}} \exp\left(-\frac{s^{1/4}}{2^{1/2}B^{1/4}}x\right) \sin\left(\frac{s^{1/4}}{2^{1/2}B^{1/4}}x - \frac{\pi}{4}\right). \quad (\text{A.9})$$

The Laplace inversion may in principle be applied to Equation (A.9) for any value of x . In

this case, it is feasible only if $x = 0$. By use of a table of Laplace transforms we find

$$\begin{aligned} y(0, t) &= -\frac{m}{2^{1/2}\Gamma(5/4)}(Bt)^{1/4}, \\ y_x(0, t) &= m, \\ y_{xx}(0, t) &= -\frac{m}{2^{1/2}\Gamma(3/4)}(Bt)^{-1/4}, \\ y_{xxx}(0, t) &= 0. \end{aligned} \tag{A.10}$$

Then, substituting $y(x, t) = m(Bt)^{1/4}Z[x/(Bt)^{1/4}]$ into Equation (A.4), and denoting $x/(Bt)^{1/4}$ by u and $dZ/du = Z'$ etc., one find the following ODE for the shape function $Z(u)$

$$Z^{(4)} - (1/4)uZ' + (1/4)Z = 0. \tag{A.11}$$

We replace the power series $Z(u) = \sum_{n=0}^{\infty} a_n u^n$ into Equation (A.11) and obtain the following recursion relation between the coefficients a_n in the usual way

$$a_{n+4} = \frac{n-1}{4(n+1)(n+2)(n+3)(n+4)} a_n. \tag{A.12}$$

The first four coefficients is calculated from relation (A.10) by using Taylor's theorem and remembering that $\partial/\partial x = (Bt)^{-1/4}(d/du)$. That is

$$a_0 = -\frac{1}{2^{1/2}\Gamma(5/4)}, \quad a_1 = 1, \quad a_2 = -\frac{1}{2^{3/2}\Gamma(3/4)}, \quad a_3 = 0.$$

Recursion relation (A.12) then determines all coefficients a_n and the solution of the original problem follows

$$y(x, t) = m(Bt)^{1/4} \sum_{n=0}^{\infty} a_n \left[\frac{x}{(Bt)^{1/4}} \right]^n.$$

Appendix B

B_splines

First we will explain the meaning of spline. A spline function consists of polynomial pieces on subintervals joined together with certain continuity conditions. Formally, suppose that $n + 1$ points x_0, x_1, \dots, x_n have been specified and satisfy $x_0 < x_1 < \dots < x_n$. These points are called *knots*.

A *spline function of degree k* having knots x_0, x_1, \dots, x_n is a function S such that:

1. On each interval $[x_{i-1}, x_i]$, S is a polynomial of degree $\leq k$
2. S has a continuous $(k - 1)$ derivative on $[x_0, x_n]$.

The cubic spline is the spline when $k = 3$. Thus

$$S(x) = \begin{cases} S_0(x) & , \quad x \in [x_0, x_1] \\ S_1(x) & , \quad x \in [x_1, x_2] \\ \vdots & \\ S_{n-1}(x) & , \quad x \in [x_{n-1}, x_n] \end{cases}$$

where S_i be the cubic polynomial that represents S on $[x_i, x_{i+1}]$.

In particular, B_splines or bell-shaped splines have several forms. One is

$$B_i(x) = \frac{1}{4h^3} \begin{cases} (x - x_{i-2})^3 & , x \in [x_{i-2}, x_{i-1}] \\ h^3 + 3h^2(x - x_{i-1}) + 3h(x - x_{i-1})^2 - 3(x - x_{i-1})^3 & , x \in [x_{i-1}, x_i] \\ h^3 + 3h^2(x_{i+1} - x) + 3h(x_{i+1} - x)^2 - 3(x_{i+1} - x)^3 & , x \in [x_i, x_{i+1}] \\ (x_{i+2} - x)^3 & , x \in [x_{i+1}, x_{i+2}] \\ 0 & , \text{ otherwise.} \end{cases}$$

which is graphed in Figure B.1.

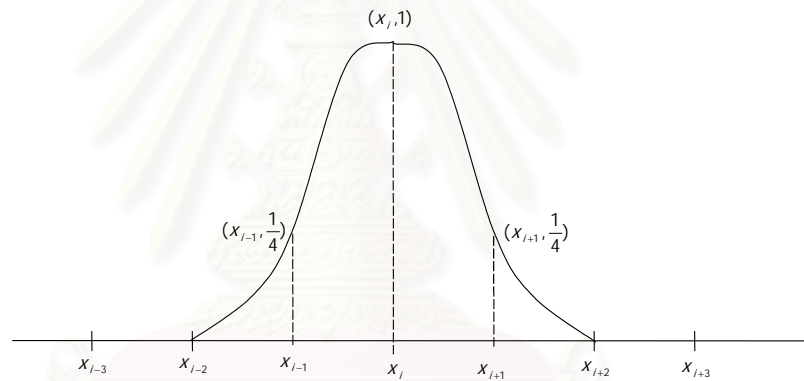


Figure B.1: Graph of $B_i(x)$.

Hence,

$$B_i(x_j) = \begin{cases} 1 & , j = i \\ 1/4 & , j = i \pm 1 \\ 0 & , \text{ otherwise.} \end{cases}$$

Now we can find $B_i'(x)$ and $B_i''(x)$:

$$B'_i(x) = \frac{1}{4h^3} \begin{cases} 3(x - x_{i-2})^2 & , \quad x \in [x_{i-2}, x_{i-1}] \\ 3h^2 + 6h(x - x_{i-1}) - 9(x - x_{i-1})^2 & , \quad x \in [x_{i-1}, x_i] \\ -3h^2 - 6h(x_{i+1} - x) + 9(x_{i+1} - x)^2 & , \quad x \in [x_i, x_{i+1}] \\ -3(x_{i+2} - x)^2 & , \quad x \in [x_{i+1}, x_{i+2}] \\ 0 & , \quad \text{otherwise} \end{cases}$$

and

$$B''_i(x) = \frac{1}{4h^3} \begin{cases} 6(x - x_{i-2}) & , \quad x \in [x_{i-2}, x_{i-1}] \\ 6h - 18(x - x_{i-1}) & , \quad x \in [x_{i-1}, x_i] \\ 6h - 18(x_{i+1} - x) & , \quad x \in [x_i, x_{i+1}] \\ 6(x_{i+2} - x) & , \quad x \in [x_{i+1}, x_{i+2}] \\ 0 & , \quad \text{otherwise.} \end{cases}$$

Thus, we can summarize them in Table B.1.

	x_{i-2}	x_{i-1}	x_i	x_{i+1}	x_{i+2}
$B_i(x)$	0	1/4	1	1/4	0
$B'_i(x)$	0	3/(4h)	0	-3/(4h)	0
$B''_i(x)$	0	3/(2h ²)	-3/h ²	3/(2h ²)	0

Table B.1

Appendix C

FDM formula

Algebraic formulae for derivative of y with respect to x :

Derivative	Type	Finite Difference Approximation
y_x	3 pt SYM	$(y_{i+1} - y_{i-1})/(2 \Delta x),$
y_{xx}	3 pt SYM	$(y_{i+1} - 2y_i + y_{i-1})/(\Delta x^2),$
y_{xxx}	5 pt SYM	$(y_{i+2} - 2y_{i+1} + 2y_{i-1} - y_{i-2})/(2 \Delta x^3),$
	5 pt ASYM	$(-y_{i+3} + 6y_{i+2} - 12y_{i+1} + 10y_i - 3y_{i-1})/(2 \Delta x^3),$
	5 pt ASYM	$(3y_{i+1} - 10y_i + 12y_{i-1} - 6y_{i-2} + y_{i-3})/(2 \Delta x^3),$
y_{xxxx}	5 pt SYM	$(y_{i+2} - 4y_{i+1} + 6y_i - 4y_{i-1} + y_{i-2})/(\Delta x^4),$
	6 pt ASYM	$(-y_{i+4} + 6y_{i+3} - 14y_{i+2} + 16y_{i+1} - 9y_i + 2y_{i-1})/(\Delta x^4),$
	6 pt ASYM	$(2y_{i+1} - 9y_i + 16y_{i-1} - 14y_{i-2} + 6y_{i-3} - y_{i-4})/(\Delta x^4).$

Note that all the above finite difference approximations are of second order.

Appendix D

Numerical inversion of Laplace transforms

The numerical inversion of Laplace transform by Stehfest [8] evaluates

$$f(t) = \frac{\ln 2}{t} \sum_{i=1}^N V_i F(s_i)$$

where

$$s_i = \frac{\ln 2}{t} i$$

and

$$V_i = (-1)^{\frac{N}{2}+i} \sum_{k=\lceil \frac{i+1}{2} \rceil}^{\min\{i, N/2\}} \frac{k^{N/2} (2k)!}{(N/2 - k)! k! (k-1)! (i-k)! (2k-i)!}$$

Note that $f(t)$ is the approximately inversed value of function $F(s)$ at time t .

For the value of N , an even positive integer, Stehfest reported after the inversion was done with 50 tested functions that the value of N should be about 18 for double

precision calculation. However, it has been shown that accurate numerical inversion of Laplace transform can be obtained using the value of N as small as 6 from [12] and [11]. Therefore, we choose $N = 6$ in this thesis.



สถาบันวิทยบริการ
จุฬาลงกรณ์มหาวิทยาลัย

VITA

Miss Patcharin Tragoonsirisak was born on October 18, 1977, in Chantaburi, Thailand. She graduated with a Bachelor degree of Science in Mathematics from Chulalongkorn University in 2000. In the same year, she was admitted into the Master Degree program in Computational Science, Department of Mathematics, Faculty of Science, Chulalongkorn University. During the study for her Bachelor's degree and Master's degree, she received a financial support from the Development and Promotion for Science and Technology talent project of Thailand (DPST).



สถาบันวิทยบริการ
จุฬาลงกรณ์มหาวิทยาลัย